Disease Models & Mechanisms 6, 689-700 (2013) doi:10.1242/dmm.010660

Elevated expression of the V-ATPase C subunit triggers JNK-dependent cell invasion and overgrowth in a *Drosophila* epithelium

Astrid G. Petzoldt[1,2,*,‡], Eva Maria Gleixner[1,2,*], Arianna Fumagalli[3], Thomas Vaccari[3,§] and Matias Simons[1,2,4,§]

SUMMARY

The C subunit of the vacuolar H^+-ATPase or V-ATPase regulates the activity and assembly of the proton pump at cellular membranes. It has been shown to be strongly upregulated in oral squamous cell carcinoma, a highly metastatic epithelial cancer. In addition, increased V-ATPase activity appears to correlate with invasiveness of cancer cells, but the underlying mechanism is largely unknown. Using the *Drosophila* wing imaginal epithelium as an *in vivo* model system, we demonstrate that overexpression of Vha44, the *Drosophila* orthologue of the C subunit, causes a tumor-like tissue transformation in cells of the wing epithelium. Overexpressing cells are excluded from the epithelium and acquire invasive properties while displaying high apoptotic rates. Blocking apoptosis in these cells unmasks a strong proliferation stimulus, leading to overgrowth. Furthermore, we show that excess Vha44 greatly increases acidification of endocytic compartments and interferes with endosomal trafficking. As a result, cargoes such as GFP-Lamp1 and Notch accumulate in highly acidified enlarged endolysosomal compartments. Consistent with previous reports on the endocytic activation of Eiger/JNK signaling, we find that V-ATPase stimulation by Vha44 causes JNK signaling activation whereas downmodulation of JNK signaling rescues the invasive phenotypes. In summary, our *in vivo*-findings demonstrate that increased levels of V-ATPase C subunit induce a Eiger/JNK-dependent cell transformation within an epithelial organ that recapitulates early carcinoma stages.

INTRODUCTION

Extra- and intracellular pH is tightly regulated by a number of proton transport systems. A prominent member is the vacuolar H^+-ATPase (V-ATPase). The proton pump is required for several cellular processes depending on the cell type and intracellular localization (Hinton et al., 2009). Through the regulation of endolysosomal acidification, the V-ATPase participates in protein degradation as well as in the control of endosomal trafficking and sorting (Hurtado-Lorenzo et al., 2006). This function was recently also suggested to be required in a number of signaling pathways important in development and cancer (Niehrs and Boutros, 2010; Yan et al., 2009; Buechling et al., 2010; Cruciat et al., 2010; Hermle et al., 2010; Vaccari et al., 2010; Hermle et al., 2013). In tumor cells, enhanced plasma membrane activity of the V-ATPase and other proton transporter strongly correlates with increased cell proliferation and invasive cell migration (Webb et al., 2011).

V-ATPases are large protein complexes that are organized into two domains: the membrane-embedded V0 domain responsible for proton translocation and the cytoplasmic V1 domain carrying out ATP hydrolysis. As a multi-subunit complex, the activity of the V-ATPase depends on the reversible assembly of the complex as well as the dynamic expression of V-ATPase subunits at different cellular membranes. Whereas most of the 15 subunits are essential structural and functional components, others function as regulatory subunits controlling assembly and subcellular localization (Forgac, 2007). One important regulatory subunit is the C subunit, termed ATP6V1C1 in mammals and Vha44 in *Drosophila*. It is the only subunit that is released into the cytosol during disassembly of the proton pump (Kane, 2000; Merzendorfer et al., 2000). Its phosphorylation by protein kinase A has been suggested to promote (re-)assembly of the V0-V1 holoenzymes (Voss et al., 2007). Furthermore, biochemical analysis has revealed that its presence stabilizes complex assembly and increases pump activity (Puopolo et al., 1992).

Among the V-ATPase subunits, ATP6V1C1 is the most upregulated gene in oral squamous cell carcinoma, a highly metastatic human cancer (Otero-Rey et al., 2008). Expression is predominant at the periphery and invasive fronts of tumors (Garcia-García et al., 2012), suggesting an important role of the C subunit in invasive growth and migration (Pérez- Sayáns et al., 2009). Other V-ATPase subunits, including the a3 and c subunits, have also been implicated in cancer metastasis (Lu et al., 2005; Nishisho et al., 2011). Moreover, it has been shown that plasma membrane activity of the V-ATPase is strongly increased in highly metastatic breast cancer cells (Sennoune et al., 2004). The general conclusion of these and other studies has been that the V-ATPase contributes to the reduced extracellular pH of tumors (Robey et

[1]Center for Systems Biology (ZBSA), University of Freiburg, Habsburgerstr. 49, 79104 Freiburg, Germany
[2]Renal Division, University Hospital Freiburg, Hugstetter Str. 55, 79106 Freiburg, Germany
[3]IFOM – FIRC Institute of Molecular Oncology, Via Adamello 16, 20139 Milan, Italy
[4]BIOSS Centre for Biological Signaling Studies, University of Freiburg, D-79104 Freiburg, Germany
*These authors contributed equally to this work
‡Present address: Institut für Biologie/Genetik, Freie Universität Berlin, Takustrasse 6, 14195 Berlin, Germany
§Authors for correspondence (thomas.vaccari@ifom.eu; matias.simons@uniklinik-freiburg.de)

Received 1 August 2012; Accepted 14 January 2013

TRANSLATIONAL IMPACT

Clinical issue

Cancer, which results from uncontrolled cell growth and tissue invasion, is the leading cause of death in the Western world. Dysregulated pH is emerging as a cancer hallmark, because in many cancers the cellular pH gradient is altered. These conditions facilitate cancer progression by promoting changes in metabolism, proliferation, migration and invasion. On the molecular level, several proton transport systems, including the V-ATPase, have been reported to show upregulated activity in cancer cells. Moreover, new evidence suggests that organellar acidification is also important for oncogenic signaling processes. However, it is not clear whether this upregulation is a cause or consequence of oncogenic transformation. To study this in more detail, cancer models that recapitulate transformation in the native tissue are needed.

Results

In this study, the authors show that overexpression of a V-ATPase subunit, Vha44, is sufficient to trigger epithelial cell overgrowth and invasion in the *Drosophila* wing disc, an *in vivo* model for tumorigenesis. Vha44, which is known as ATP6V1C1 in mammals, is strongly upregulated in human oral squamous cell carcinoma. The authors demonstrate that most Vha44-induced phenotypes can be blocked by JNK inhibition, indicating that the JNK signaling pathway is central to the transformation process *in vivo*. By contrast, the phenotype is enhanced by coexpression of an oncogenic form of Ras. Ectopic Vha44 expression was shown to increase the activity of the V-ATPase in intracellular organelles, leading to severe defects in endolysosomal degradation. As JNK signaling has been shown to be activated in endosomes, such endolysosomal defects might have a crucial role in oncogenic transformation.

Implications and future directions

Endosomal signaling is an emerging feature in signal transduction biology. Many developmental signaling pathways, including Notch, Wnt and JNK, require acidified organelles for proper signaling. The main conclusion arising from this work is that endosomal acidification via the V-ATPase is more important for oncogenesis than anticipated. The quest for new cancer therapies in the form of inhibitors of the V-ATPase should therefore include molecules that are able to target the endosomal pool of the V-ATPase. Small-molecule inhibitors against endosomal V-ATPases might be particularly useful for tumors that depend on the synergistic activation of Notch, Wnt and JNK signaling. Screening for genetic modifiers as well as testing of combinatorial therapies could be performed using the *Drosophila* model established here. The main advantage of this model is that oncogenic transformation is induced genetically within the native epithelium.

al., 2009; Webb et al., 2011). V-ATPase inhibitors have therefore been tested in human cancer trials with the rationale to lower tumor acidity and to improve patient outcome (Otero-Rey et al., 2008; Hinton et al., 2009; Fais, 2010; Webb et al., 2011). Most experimental data concerning the role of V-ATPase subunits in tumorigenesis has been obtained by using xenografts or cultured tumor cell lines separated from their tissue microenvironment (Sennoune et al., 2004; Lu et al., 2005; Nishisho et al., 2011). The question whether changes in cellular pH are cause or consequence of cancerous transformation therefore largely remains unanswered. Furthermore, it is not known whether altered V-ATPase function might impact cell behavior via the regulation of signaling pathways.

Here, we report on the oncogenic properties of the C subunit of the V-ATPase, Vha44, in the fruit fly *Drosophila melanogaster*. *Drosophila* imaginal discs are excellent model tissues for studying the function of individual oncogenes and tumor suppressors but also the cooperativity of genes in native cellular environments (Vidal et al., 2006; Halder and Mills, 2011). By contrast to xenografts or cultured cancer cell lines, the mutational load can be precisely controlled, allowing the genetic requirements of cell transformation to be analyzed within the tissue of origin. Moreover, because tumor cells are genetically produced, mechanical disruption of cells and of the extracellular matrix is avoided. Using the wing disc as a model epithelium, we show that the overexpression of Vha44 is sufficient to trigger invasive cell behavior in the epithelial wing disc tissue. Our data suggest that ectopic Vha44 expression increases vesicular acidification, impairs endolysosomal degradation and induces a TNF/Eiger- and JNK-dependent transformation program.

RESULTS

Increased Vha44 expression causes cell invasiveness

Overexpression of Vha44 was targeted to the patched (*ptc*) expression domain of the larval wing disc epithelium using the GAL4/UAS expression system. This domain constitutes a narrow stripe at the anterior-posterior (AP) boundary, in which expression is highest at the boundary-facing side of the stripe (Fig. 1A-E). Expression of both HA-tagged and untagged Vha44 caused a striking unidirectional migration of the cells from the anterior *ptc* stripe into the posterior compartment (Fig. 1B,D; supplementary material Fig. S1A,B). Additional expression of monomeric red fluorescent protein (mRFP) confirmed the identity of the invading cells as originating from the *ptc* stripe (Fig. 1B,B′). In control discs, mRFP expression was always confined within the *ptc* stripe (Fig. 1A,C), consistent with the role of the AP boundary in preventing mixing of cells (Landsberg et al., 2009). x-z axis projection revealed that migration took place on the basal side of the wing epithelium (Fig. 1D). These results suggest that cells close to the boundary are extruded basally and then move towards the posterior compartment. Basal invasion into the neighboring compartment was also seen by Vha44 overexpression in other compartments of the wing disc such as the dorsal part using *apterous (ap)*-GAL4 (supplementary material Fig. S1A,D). Therefore, we conclude that Vha44 overexpression can trigger invasion in different regions of the disc epihelium.

Blocking apoptosis unmasks overgrowth caused by Vha44

Basal extrusion of epithelial cells in *Drosophila* tissue is often accompanied by apoptosis (Vidal et al., 2006; Igaki et al., 2009; Marinari et al., 2012). Accordingly, we observed that most of the extruded cells displayed pyknotic nuclei suggestive of apoptotic cell death (not shown). Further investigation revealed that, unlike mRFP-expressing control cells, a significant fraction of the invasive cells were positive for cleaved Caspase 3 (Cas3) as well as TUNEL labeling (Fig. 1F,G; supplementary material Fig. S2A,B). Apoptosis was highest at the AP boundary and in the invasive front. This suggests that cells were displaced into the basal extracellular matrix (ECM) at the boundaries due to apoptosis and then migrated into the posterior compartment. Consistent with previous results, we further verified that, unlike Vha44, the induction of apoptosis by overexpression of a pro-apoptotic protein is not sufficient to cause cell migration (supplementary material Fig. S2C,D; Vidal et al., 2006). This indicates that additional mechanisms are involved in the invasive behavior.

Next, we coexpressed the baculovirus protein p35, which acts as a strong suppressor of apoptosis by inhibiting Cas3 function (Hay et al., 1994). As a result, we observed no apoptosis and basal exclusion, but nevertheless the *ptc* stripe appeared broadened and

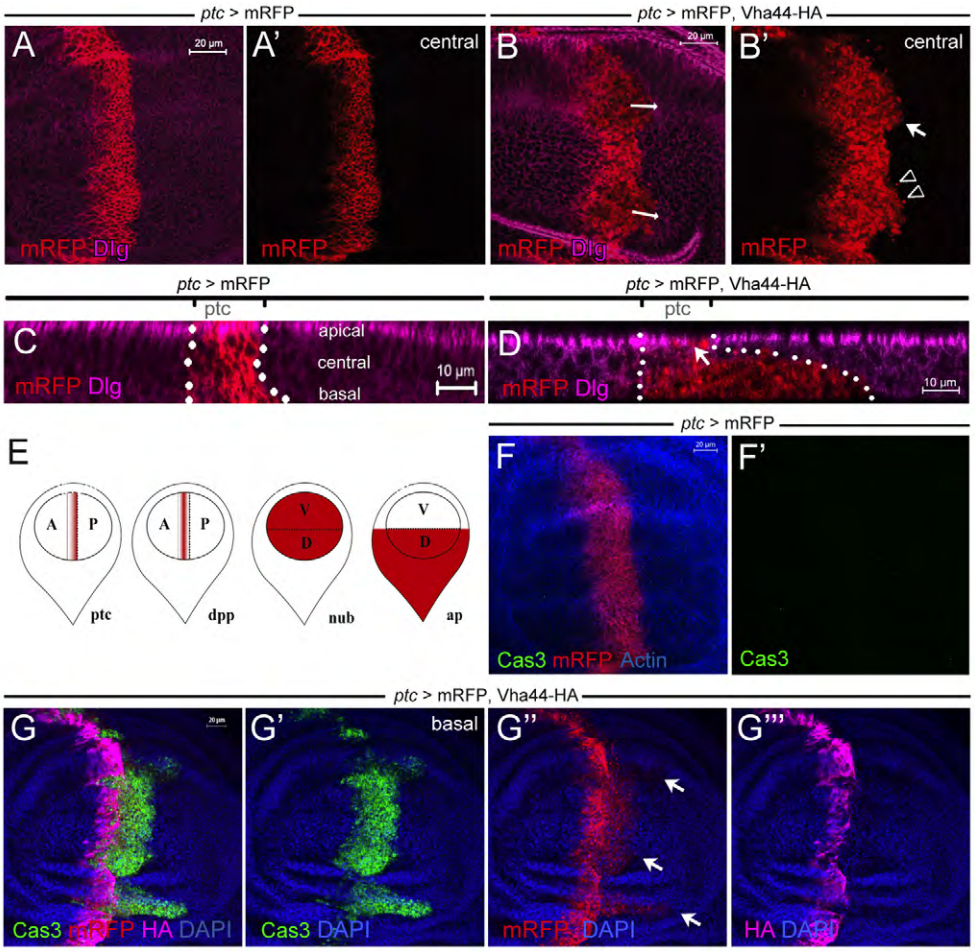

Fig. 1. Vha44 overexpression causes invasive migration and apoptosis at the AP boundary of the wing disc. (A,B) *ptc*-GAL4 is used to drive expression of mRFP (A,A′) and mRFP/Vha44-HA (B,B′) in an anterior stripe at the boundary to the posterior compartment. Expression is highest close to the boundary. Staining for Discs large (Dlg) visualizes the outline of individual cells and the whole tissue. Invasion is most prominent at dorsal and ventral parts of the wing pouch (arrowhead indicates single cells migrating; arrow indicates cell clusters migrating in B′). (C,D) Invading cells (below dotted line) move at the basal side of the epithelium as seen in the x-z projection. Dlg is missing right next to the boundary, most probably due to basal extrusion and loss of apico-basal polarity (arrow in D). (E) Schematic drawings of the wing disc and the respective expression domains for the GAL4 drivers used throughout this study, in red. (F,G) Whereas mRFP expression does not induce Cas3 reactivity (F,F′), coexpression of Vha44-HA leads to Cas3-positive cells in the *ptc* stripe (G′). As demonstrated by the mRFP signal (G″), Vha44-expressing cells are of anterior identity. Note that the HA tag is hardly visible in the invasive Cas3- and mRFP-positive front due to the apoptotic cleavage (G‴; see also supplementary material Fig. S1 for further clarification). It can therefore be used to mark the original *ptc* stripe. In images with higher exposure, the HA signal is also visible in the invasive front (see also supplementary material Fig. S1A).

irregular (Fig. 2A,B; supplementary material Fig. S2E,F). Staining for phospho-histone 3 (PH3) revealed increased proliferation in the *ptc* stripe in Vha44/p35- but not in mRFP/p35-expressing control cells (Fig. 2C,D). Expressing Vha44 in the *ap* or *nubbin* (*nub*) compartments, encompassing most of the wing disc or wing pouch, respectively, led to overgrowth even in the absence of p35, as shown by the increased size of the compartments and the protruding bulges at the wing disc edges (Fig. 2F,G; supplementary material Fig. S1C). We therefore conclude that Vha44 overexpression promotes proliferation, an effect that is masked by strong apoptosis at the AP boundary.

Vha44 cooperates with oncogenic Ras

The phenotypes observed upon Vha44 overexpression are reminiscent of the cellular transformation occurring during tumorigenesis. Thus, we next investigated whether ectopic Vha44 expression activates oncogenic signaling pathways previously reported to mediate cell invasion and overgrowth in the wing disc (Vidal et al., 2006; Singh et al., 2010). Silencing the Src inhibitor Csk with a previously validated RNAi line did not significantly increase the level of Vha44-induced migration (Vidal et al., 2006; supplementary material Fig. S3A-D). Neither did we find a significant activation of Abl in the Vha44-expressing cells (supplementary material Fig. S3E). In contrast, the co-overexpression of Vha44 and RasV12, the oncogenic form of Ras, led to a strong increase in cell migration compared with overexpressing Vha44 and the control protein mRFP (Fig. 3B-D). Coexpressing RasV12 and Vha44 also caused a synergistic effect with regard to overgrowth (Fig. 3F-H). Because RasV12 expression alone did not lead to any invasion or overgrowth (Fig. 3A,E), these

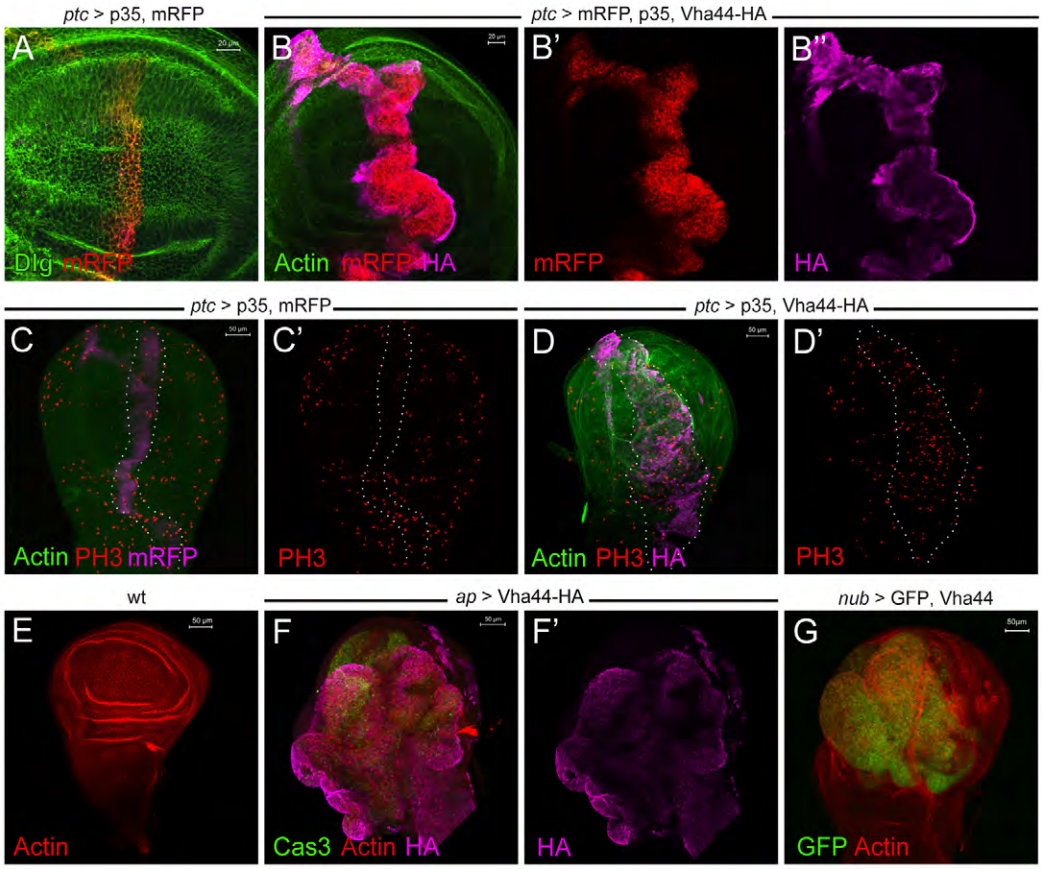

Fig. 2. Vha44 overexpression causes overgrowth. (A,B) Although the coexpression of p35 and mRFP does not lead to any overt phenotypes or apoptosis (A), additional expression of Vha44-HA causes an expansion of the ptc stripe (B,B′,B″). (C,D) Phospho-histone 3 (PH3) staining reveals an increased proliferation rate in the *ptc* domain (marked by dotted lines in D and D′), but not in the control ptc stripe expressing p35 and mRFP (marked by dotted lines in C and C′). (E-G) *Ap*-GAL4- (F,F′) and *nub*-GAL4-mediated (G) overexpression of Vha44 causes overgrowth in the dorsal compartment and wing pouch, respectively. Cas3-positive cells are also detectable (F). For comparison, a wild-type disc stained with phalloidin is shown (E).

results indicate that Vha44 cooperates with oncogenic Ras in invasion and overgrowth.

Overexpression of Vha44 lowers endolysosomal pH and alters V-ATPase subunit levels

To understand the cellular mechanism by which Vha44 overexpression induces this complex tumor-like phenotype, we first examined the subcellular localization of overexpressed Vha44 in wing discs. Consistent with the reported localization of V-ATPase (Feng et al., 2009), endogenous and overexpressed Vha44 was mainly found in intracellular organelles but also at the plasma membrane of epithelial wing cells (supplementary material Fig. S4B-D). A substantial fraction of these organelles were positive for the late endosomal marker Rab7 (supplementary material Fig. S4D). To investigate the effects of Vha44 overexpression on V-ATPase function, we applied the acidotrophic fluorescent dye LysoTracker to isolated live wing discs overexpressing Vha44 under *ptc*-GAL4. We observed a strong accumulation of LysoTracker in the *ptc* stripe but not in the neighboring wild-type cells or in control cells (Fig. 4A,B). This indicates that organellar acidification is increased in Vha44-expressing cells. Blocking V-ATPase activity with the specific inhibitor Concanamycin A resulted in the complete loss of the LysoTracker labeling, indicating that the Vha44-mediated increase in organellar acidification is due to enhanced V-ATPase function (Fig. 4C). In addition, we found that overexpression of another V-ATPase subunit, Vha100-1, did not alter Lysotracker incorporation or cause invasion and overgrowth phenotypes (supplementary material Fig. S5A-C). In line with the proposed V-ATPase assembly function for Vha44, these results suggest that unlike Vha100-1, Vha44 is sufficient to cause association of V0 and V1 subcomplexes, thus increasing the amount of functional holoenzymes within membranes of intracellular organelles. Accordingly, using a GFP insertion in the genomic locus of Vha16-1, we found enhanced levels of the V0 component Vha16-1-GFP upon Vha44 overexpression (Fig. 4D). By contrast, a GFP insertion in VhaSFD was downregulated upon Vha44 overexpression (Fig. 4E). The reason for this downregulation is unclear. However, as VhaSFD (or H subunit) has been reported to inhibit ATP hydrolysis of the unassembled V1 sector (Jefferies and Forgac, 2008; Diab et al., 2009), its reduction upon Vha44 overexpression might be consistent with increased pump assembly.

To test whether increased proton transport is the cause of the observed tissue alterations, we overexpressed the sodium-proton exchanger Nhe2. This multi-transmembrane protein translocates protons across membranes in the same direction as the V-ATPase and has been shown to localize to the plasma membrane and endosomes (D'Souza et al., 1998). We found that Nhe2-YFP overexpression caused weaker but very similar phenotypes compared to Vha44: invasion, apoptosis and overgrowth and increased organellar acidification, (supplementary material Fig. S6A-D). By co-staining with Avl and Rab7, we confirmed that a pool of overexpressed Nhe2-YFP localized to early and late endosomal compartments (supplementary material Fig. S6E,F). Taken together, these results suggest that increased endolysosomal

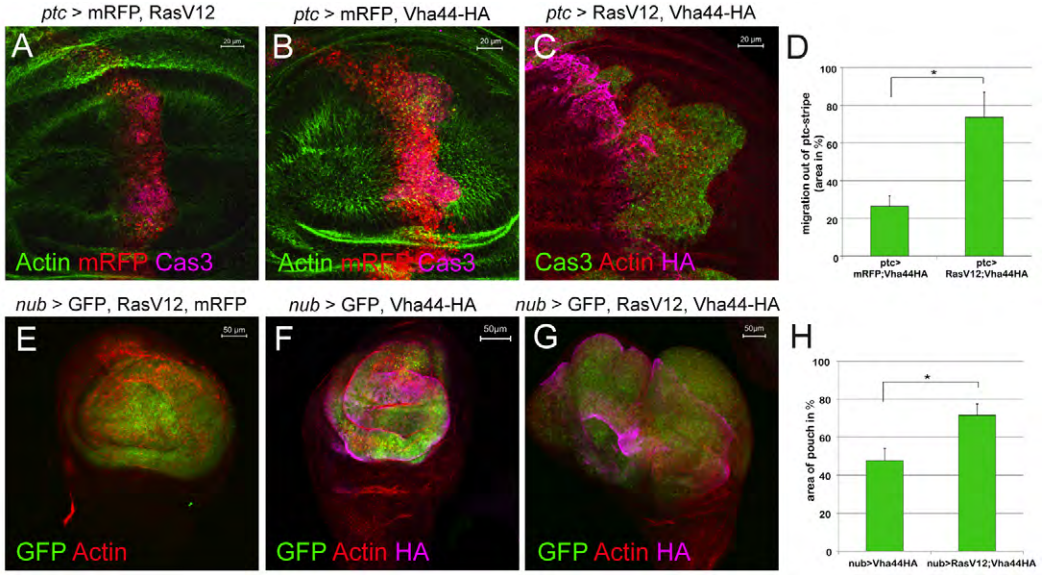

Fig. 3. Vha44-induced invasion and overgrowth is enhanced by RasV12. (A-C) RasV12/mRFP coexpression does not lead to significant invasion phenotypes (A). Co-overexpression of the oncogenic form of Ras, RasV12 and Vha44 (C) increases the extent of migration seen in Vha44/mRFP coexpression (B). (D) Quantification of the ratios (in %) between the areas of invaded Cas3-positive cells and the areas of the original *ptc* stripe (n=9). Data represent the mean ± s.d.; Student's t-test (*P<0.01). (E-H) The expression of mRFP and RasV12 with *nub*-GAL4 does not lead to overgrowth. Vha44/mFRP overexpression under *nub*-GAL4 causes overgrowth (F), which is significantly increased in the presence of RasV12 (G). (H) Quantification of disc diameters (n=6). Data represent the mean ± s.d.; Student's t-test (*P<0.0001).

acidification might be sufficient for invasion and overgrowth phenotypes.

Endolysosomal proteolysis is impaired in Vha44-expressing cells

V-ATPase-dependent acidification has been linked to endosomal sorting and lysosomal degradation (Hurtado-Lorenzo et al., 2006). To study these membrane trafficking processes, we first expressed a GFP-Lamp1 fusion construct under the ubiquitous *tubulin* promoter. In *Drosophila* cells, the LAMP1-derived cytoplasmic tail is sufficient to target this fusion protein from the Golgi to late endosomes and lysosomes, where hydrolases degrade GFP (Rohrer et al., 1996; Pulipparacharuvil et al., 2005). Whereas GFP-Lamp1 was hardly detectable in the neighboring tissue and in mRFP-expressing control cells (Fig. 5A-C), overexpression of Vha44 (with and without p35) caused a severe accumulation of GFP-Lamp1 in the *ptc* stripe (Fig. 5B,C). GFP-Lamp1 partially colocalized in enlarged organelles with the late endosomal marker Rab7 and Lysotracker (Fig. 5D,E), giving rise to a ring-like structure with luminal GFP signal and Rab7 signal at the limiting membrane (inset in Fig. 5D). Generally, there seemed to be an irregular localization pattern for Rab7 in the Vha44-expressing *ptc* stripe with accumulations in enlarged compartments (Fig. 5F,G). Together, these data suggest that Vha44 overexpression impairs endolysosomal degradation leading to cargo accumulation in enlarged late endosomes and/or lysosomes.

Notch accumulation in acidic compartments does not significantly alter Notch signaling in Vha44-expressing cells

Endocytic activation and/or impaired degradation of signaling receptors have been implicated in sustained tumor growth and invasion. In *Drosophila*, oncogenic Notch and c-jun N-terminal kinase (JNK) signaling has been demonstrated to occur in endosomes (Vaccari et al., 2008; Igaki et al., 2009; Vaccari and Bilder, 2005; Wilkin et al., 2008; Rodahl et al., 2009; Hori et al., 2011). Therefore, we investigated the role of Notch and JNK signaling in Vha44-induced transformation. Consistent with alterations of protein trafficking and degradation upon ectopic Vha44 expression, we found an accumulation of the transmembrane receptor Notch in the lumen of enlarged late endosomes (Fig. 5I,J). In addition, we found a significant colocalization of Notch-YFP with LysoTracker (Fig. 5M,N). To monitor directly whether Notch is degraded in Vha44-expressing cells, we applied an antibody against the extracellular domain of Notch (NECD) onto live wing discs. Notch was found at the cell surface at t=0 hours in Vha44-expressing cells (Fig. 5K). In contrast, after 5 hours, the receptor accumulated in intracellular compartments in Vha44-cells (Fig. 5L). These results indicate that, similarly to GFP-Lamp1, Notch accumulates in Vha44-overexpressing cells due to reduced endolysosomal degradation.

Previous studies have shown that Notch activation requires V-ATPase activity (Yan et al., 2009; Vaccari et al., 2010; Hermle et al., 2013). We therefore tested the status of Notch signaling activation in cells overexpressing Vha44. We found that in Vha44-expressing cells expression of the Notch signaling reporter *E(Spl)mβeta-lacZ* was well detectable in areas in which Notch signaling is normally low, such as the presumptive vein regions of the disc. However, it was not as high as in peak signaling portions of the disc, such as the presumptive wing margin (supplementary material Fig. S7A-D). Accordingly, overexpression of Vha44 resulted in both Notch gain- and loss-of-function phenotypes in adult wings (supplementary material Fig. S7G-J). Finally, quantitative real-time PCR (qPCR) demonstrated no significant change in *E(Spl)mβeta* expression in wing discs expressing Vha44 with *nub*-GAL4

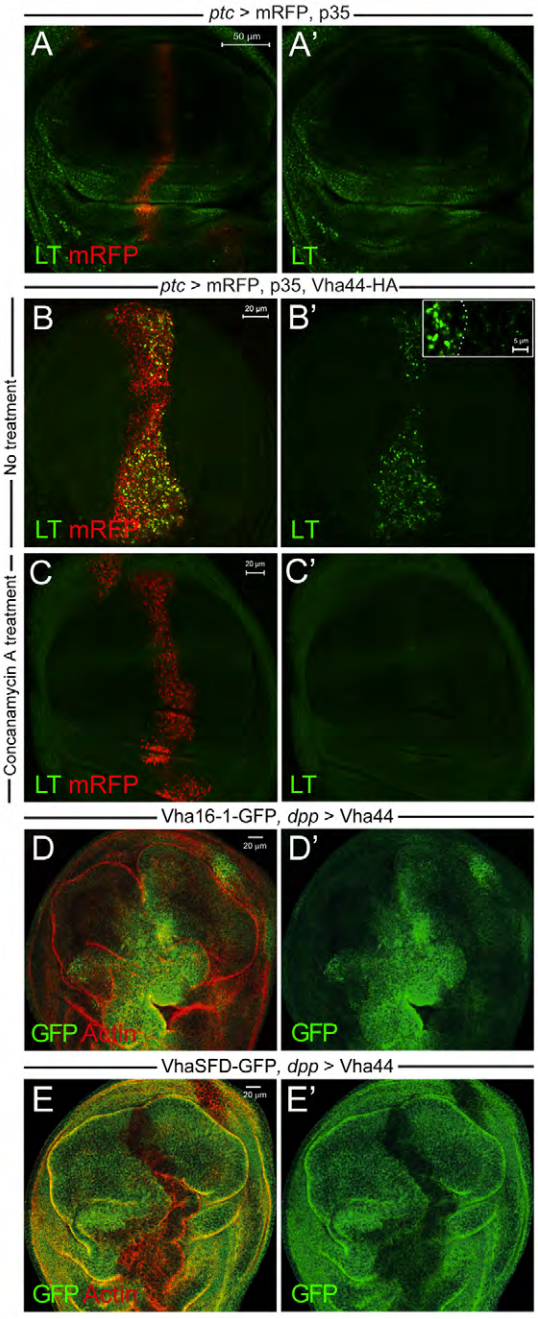

Fig. 4. Vha44 expression increases organellar acidity and alters V-ATPase subunit levels. (A-C) Although LysoTracker (LT) uptake is normal in ptc stripes expressing mRFP and p35 (A,A′), LT accumulated strongly within intracellular puncta in cells overexpressing Vha44-HA, mRFP and p35 (B,B′ and inset in B′; cells marked with mRFP in B). To reduce dye uptake due to removal of apoptotic cells by acidic phagosomes of hemocytes or neighboring cells, the anti-apoptotic p35 was coexpressed in these experiments. LT uptake by cells outside the *ptc* stripe was also seen, but is hardly detectable at the laser intensity shown in B and B′. (C) Pre-incubation with the V-ATPase inhibitor Concanamycin A abolishes all LT signal in the *ptc* stripe. (D,D′) Endogenous Vha16 (tagged with GFP) expression is enhanced in cells overexpressing Vha44 with *dpp*-GAL4. (E,E′) By contrast, VhaSFD-GFP expression is decreased. Note that when Vha44 expression is targeted to the *dpp* domain, then there is also overgrowth, because there are less boundary effects compared to the *ptc* domain (see also Fig. 1E).

(supplementary material Fig. S7K). This suggests that despite Notch accumulation in acidified organelles, there is no major alteration of Notch pathway activation in Vha44-overexpressing cells compared with wild-type cells.

Eiger/JNK signaling is required for Vha44-dependent invasion and overgrowth

In contrast to Notch signaling, the qPCR revealed increased expression of the JNK signaling inhibitor and target gene *puckered* (*puc*; supplementary material Fig. S7K). We therefore monitored JNK activity in the Vha44-expressing cells by immunostaining for the activated phosphorylated form of JNK (pJNK) and by assessing *puc* expression using the transcriptional reporter *puc-lacZ*. Both, pJNK and *puc-lacZ* levels were increased in Vha44-expressing cells but not in mRFP-expressing control cells (Fig. 6A,B; supplementary material Fig. S8A,B), indicating that JNK signaling is activated. Similar results were obtained for Nhe2 (supplementary material Fig. S6B). Accordingly, we found that the expression of Hep^{CA}, the activated form of JNKK kinase, is sufficient to drive invasion (supplementary material Fig. S8D). A further readout for upregulated JNK activity is increased expression of Matrix Metalloproteinase-1 (MMP1). MMPs are essential downstream targets of JNK that control invasive migration via basal membrane degradation (Uhlirova and Bohmann, 2006; Vidal et al., 2006). Consistent with JNK activation, we found increased MMP1 levels basally in the domain of Vha44 but not mRFP expression (Fig. 6C,D). We also observed a clear loss of the basal membrane components collagen IV and laminin (Fig. 6E; supplementary material Fig. S8F). These effects were abolished by the coexpression of p35 (Fig. 6F), indicating that the degradation of the basal membrane is linked to apoptosis and basal extrusion of cells. Taken together, these results suggest that excess Vha44 leads to JNK activation, resulting in apoptosis as well as MMP1 upregulation and ECM degradation, which might be a prerequisite for basal extrusion and invasion.

To test whether inhibition of JNK signaling is not only necessary but also sufficient to drive invasive behavior, we coexpressed Puc and Vha44. Inhibition of JNK signaling rescued apoptosis as well as the migration and proliferation phenotypes (Fig. 6G,G′). A similar suppression of apoptosis and proliferation was observed when coexpressing Basket (Bsk)-DN, a dominant-negative form of the *Drosophila* orthologue of JNK, with *ap*-GAL4 (Fig. 6H,H′). Consistent with these results, we found that the activation of JNK signaling resulting from expression of *puc-lacZ*, a hypomorphic allele of the inhibitor Puc, increased the invasion phenotype (Fig. 6B, compare with 6D). Finally, we tested the contribution of Eiger, the only *Drosophila* orthologue of the TNF-α ligand and potent activator of JNK signaling (Igaki et al., 2002; Moreno et al., 2002), by expressing Vha44 in a mutant *eiger* background. Loss of both *eiger* copies strongly suppressed apoptosis, invasion and overgrowth of Vha44-expressing cells (Fig. 6I,J). Together, these results demonstrate that Eiger/JNK signaling is both necessary and sufficient for Vha44-dependent invasion and overgrowth (for a model see Fig. 7).

DISCUSSION

Excess Vha44 leads to tumorigenesis in the wing disc

Increasing evidence suggests that pH alterations significantly affect cancer features including sustained growth, tissue invasion,

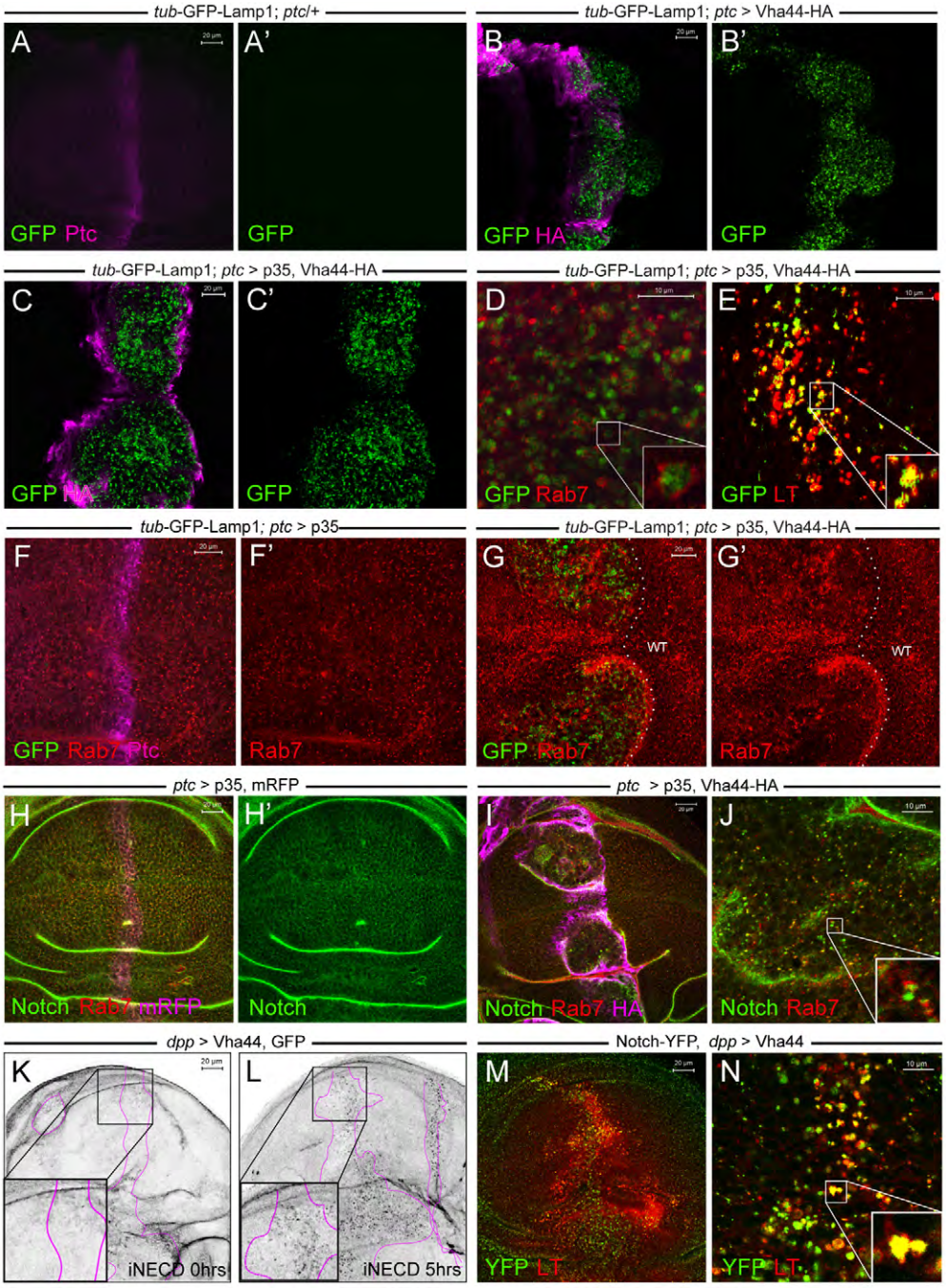

Fig. 5. Endolysosomal degradation is impaired in Vha44-expressing cells. (A-G) Luminal GFP is directed from the Golgi via early and late endosomes to the lysosomes for degradation in all panels to assess defects in endolysosomal degradation. (A,B) GFP-Lamp1 (ubiquitously expressed with a *tub* promoter) is hardly detectable in control discs (A,A′) and outside the ptc stripe (B,B′), but accumulates in Vha44-expressing cells (B,B′). (C,C′) The accumulation also occurs upon p35 coexpression. (D,E) Accumulated GFP-Lamp1 partially colocalizes with the late endosomal marker Rab7 (D) and LysoTracker (LT; E) in enlarged endosomes of the p35/Vha44-HA-expressing *ptc* stripe. The inset in D shows that, whereas Rab7 localizes to the cytosolic side of enlarged 'ring' endosomes, the GFP in GFP-Lamp1 is luminal. LysoTracker, on the other hand, shows a significant overlap with the GFP signal (inset in E). (F) Rab7 looks normal in p35-overexpressing cells. (G) Upon Vha44-HA overexpression, Rab7 becomes irregular and accumulates in enlarged compartments (*ptc* stripe is marked here by GFP-Lamp1 accumulation). Note also that the *ptc* stripe is broadened and abnormally folded due to p35 coexpression. (H) Notch localizes to membranes and intracellular puncta in a control wing disc expressing p35 and mRFP. (I) In Vha44-HA expressing cells, Notch accumulates in enlarged intracellular puncta. A higher magnification in I′ shows colocalization of Notch and Rab7. The inset highlights one enlarged compartment positive for both Notch and Rab7. (K,L) Notch antibody targeting the extracellular domain of Notch was applied to live wing discs. Compared to initial labeling (*t*=0 hours in K) internalized anti-Notch (iNECD) accumulates in the Vha44 expression domain (marked by pink lines, based on GFP coexpression) after culturing for 5 hours. In neighboring wild-type tissue, iNECD signal is lost because of lysosomal degradation (L). This suggests that Notch degradation is impaired in Vha44-expressing cells. (M,N) A pool of Notch-YFP that accumulates in Vha44-expressing cells is present in acidified LysoTracker-positive compartments. The inset in N shows overlap of Notch-YFP and Lysotracker in enlarged compartments.

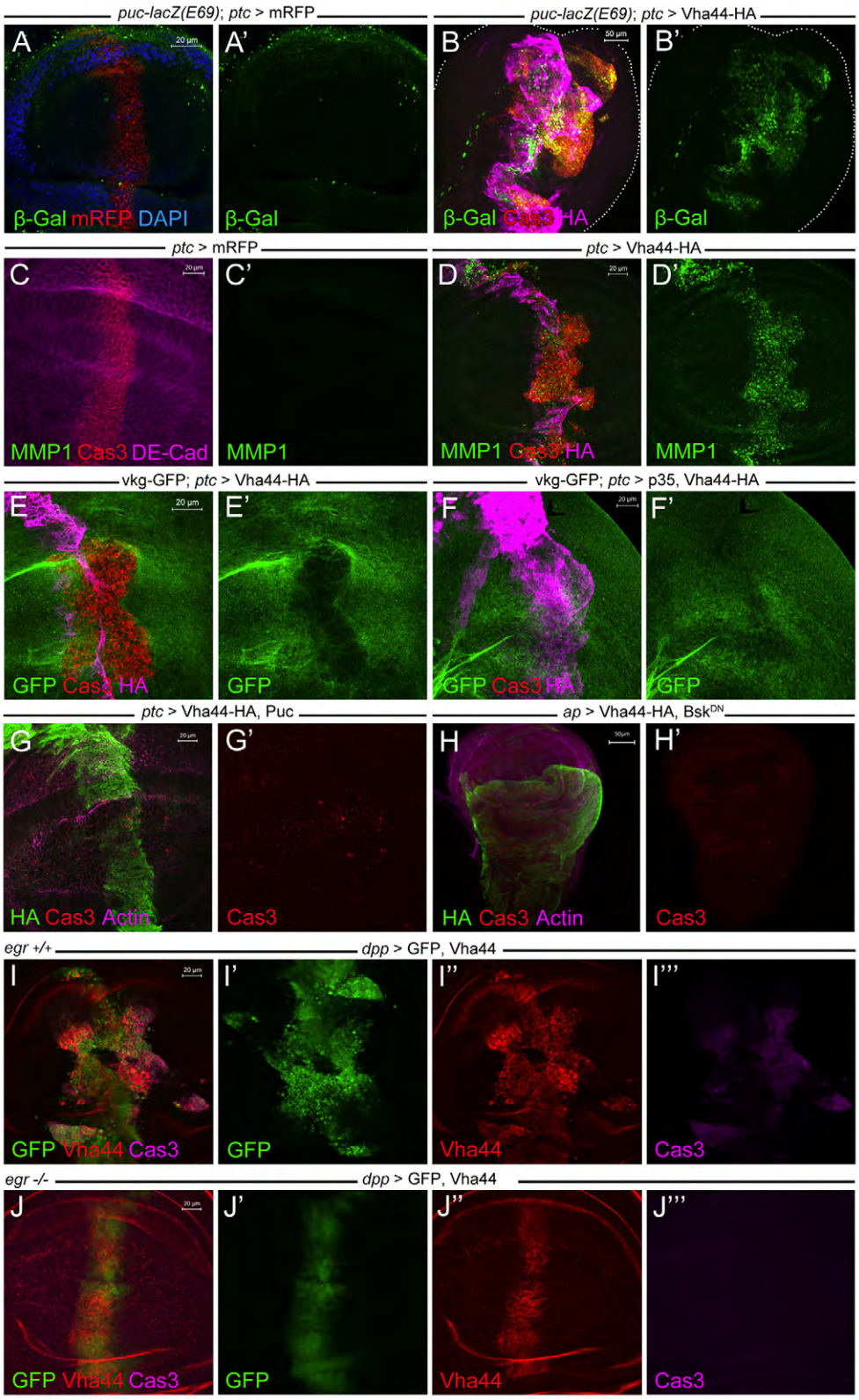

Fig. 6. Vha44-mediated transformation requires the JNK signaling pathway. (A,B) The *puc-lacZ* reporter is strongly activated in Vha44-expressing cells when stained with anti-β-gal (B,B′). As the *puc (E69)-lacZ* insertion partly disrupts gene function of the JNK inhibitor *puc*, invasion and overgrowth is enhanced in this genetic background (compare with previous examples of Vha44-induced invasion or D). No β-gal staining is detected upon expression of mRFP alone (A,A′). (C,D) *Ptc*>Vha44-HA (D,D′), but not mRFP (C,C′), strongly upregulates MMP1 expression. (E) The gene trap viking (vkg)-GFP visualizes collagen IV and was used to monitor ECM degradation in the *ptc* stripe expressing Vha44-HA (E′). (F,F′) Vkg-GFP is unaffected upon p35 coexpression, which abolishes Cas3-positive cells (F). Strong Cas3 reactivity is shown without p35 (E). (G) Coexpression of the negative regulator Puc suppressed Vha44-induced apoptosis and cell invasion. Unlike p35 (in Fig. 2B), overgrowth is also not seen. (H) The dominant-negative form of JNK, Bsk-DN, also suppresses overgrowth and apoptosis of *ap*>Vha44. (I,J) Vha44 expression using *dpp*-GAL4 also leads to overgrowth and migration out of the *dpp* expression domain (I,I′). Removing two copies of the *eiger* gene completely suppresses overgrowth, migration and apoptosis (J-J‴).

metastatic potential and chemoresistance (Stock and Schwab, 2009; Webb et al., 2011). Whether the effect of dysregulated pH on cancer progression is a cause or consequence for the development of these tumor traits has been difficult to address using traditional approaches such as xenografts or cultured cancer cell lines. In addition, because pH alterations ultimately affect multiple cellular processes, it is unclear what process is required for tissue transformation.

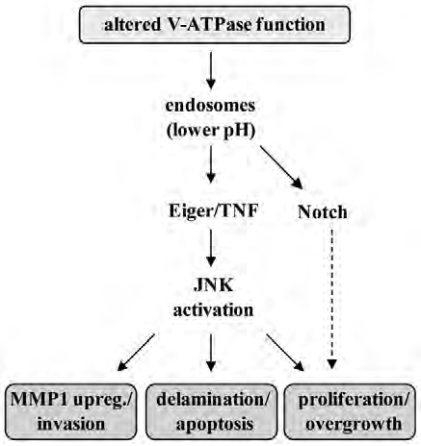

Fig. 7. Model for the proposed effects of increased vesicular V-ATPase activity. Lower pH in endosomes and defective lysosomal degradation leads to trapping of Notch and, presumably, to increased JNK signaling via its ligand Eiger. Downstream are various processes important for cellular transformation in the native epithelium. The Notch receptor also accumulates intracellularly in Vha44-expressing cells. However, Notch signaling is not significantly activated. Therefore, the contribution of Notch to the transformation phenotypes is less prominent than for JNK signaling (dotted arrow).

Drosophila imaginal discs are excellent model tissues for studying the impact of transforming events in the native epithelium (Vidal et al., 2006; Halder and Mills, 2011). Here, we have shown that overexpression of the V-ATPase subunit Vha44 in different compartments of the epithelial wing disc is sufficient to induce tumor-like transformations. Cells overexpressing Vha44 overproliferate, giving rise to protruding cell masses. In addition, they display increased apoptotic rates and basal invasion, which is facilitated by ECM degradation. Both overgrowth and invasion are increased by oncogenic Ras and inhibited by downregulation of Eiger/JNK signaling, demonstrating that the latter pathway is a key driver of cellular transformation in our tumor model.

Enhanced V-ATPase activity alters endosomal trafficking

How does Vha44 induce such a complex tumor-like phenotype? In line with the proposed role of the C subunit as an assembly and disassembly regulator (Puopolo et al., 1992; Huss et al., 2011), we have found that Vha44 overexpression leads to enhanced uptake of LysoTracker in wing epithelial cells. This effect is reversed by pharmacological V-ATPase inhibition and mimicked by overexpression of a different proton exchanger, suggesting that Vha44-overexpressing cells possess increased proton pump assembly and activity at intracellular membranes. Although the overexpression of another V1 subunit also increased vacuolar acidity in yeast (Hughes and Gottschling, 2012), the overexpression of a transmembrane V0 subunit, Vha100-1, did not lead to additional LysoTracker uptake. This suggests that excess cytosolic V1 components are more effective in enhancing V-ATPase assembly and, thus, activity.

We expected that increased pump activity would result in more lysosomal degradation. In contrast, we found the opposite. GFP-Lamp1 and Notch accumulated in enlarged late endosomal compartments in which Notch degradation is impaired. A similar combination of increased acidification and decreased proteolysis has been observed in cells deficient for the lysosomal transporter Spinster (Rong et al., 2011). How endosomal sorting and transport become blocked upon increased acidification is currently unclear. An interesting possibility is that changes in luminal pH might alter the binding properties of proteins and lipids at the cytosolic side of the endosomes (Hurtado-Lorenzo et al., 2006). Indeed, in mammalian cells, the acidification by the V-ATPase was shown to promote transport towards lysosomes by recruiting the GTPase ARF6 (and possibly Rab7 as suggested here) to early endosomes (Hurtado-Lorenzo et al., 2006). Therefore, excessive acidification might alter endosomal maturation and cargo progress towards functional lysosomes.

How could endosomal trapping of signaling receptors promote cellular transformation?

Our results are in accordance with previous findings demonstrating that the inhibition of lysosome formation in *dor*, *car*, *tsg101* and *vps25* mutants can cause tumor growth and invasion in the fly (Moberg et al., 2005; Thompson et al., 2005; Vaccari and Bilder, 2005; Chi et al., 2010). These mutations block the maturation of late endosomes to lysosomes at different levels, similarly causing signaling receptor accumulation. Furthermore, the progression of *vps25*-dependent tumors was shown to be suppressed by mutants for V-ATPase subunits, suggesting that oncogenic signaling requires low intraluminal pH (Vaccari et al., 2010). It is therefore possible that a decreased luminal pH might promote clustering or conformational changes of receptors that alter recruitment of cytosolic signal transducers. The activation of Eiger/JNK signaling, the key pathway in our tumor model, has also been linked to endosomes (Igaki et al., 2009). However, at this point it is unclear to what extent acidity contributes to the activation of Eiger, its receptor Wengen and/or the phosphorylation of JNK (Igaki et al., 2011). For the canonical Wnt [or Wingless (Wg)] pathway, it has been shown that the receptor complex, consisting of Frizzled and LRP6, can directly bind to a V-ATPase subunit and that phosphorylation of LRP6, a prime event in the signaling cascade, occurs upon entry into acidic endosomes (Buechling et al., 2010; Cruciat et al., 2010; Hermle et al., 2010). In the case of the Notch receptor, acidification might promote the intramembraneous S3 cleavage by presenilins (Vaccari et al., 2010). Alternatively, the reduced proteolysis rate in a disturbed endolysosomal pathway might increase the time of transit of receptors in signaling-competent endosomes, leading to sustained signaling. Further investigation is therefore needed to elucidate the precise mechanisms by which signaling receptors and their downstream transducers, particularly within the JNK signaling pathway, become activated in acidified compartments.

The epithelial environment influences the transformation process

The induction of cellular transformation in a patch of cells within an epithelium, as described here, elicits a myriad of cell-autonomous and non-cell-autonomous responses. Epithelial neighbors and recruited inflammatory cells release both proliferative and apoptotic stimuli that strongly influence tumor growth (Cordero et al., 2010). Transformed cells that become apoptotic might further stimulate proliferation of the surviving ones by releasing growth-promoting morphogens such as Wg and Dpp (Huh et al., 2004; Pérez-Garijo et al., 2004; Ryoo et al., 2004; Morata

et al., 2011). Accordingly, we observed that Wg strongly accumulates in parts of the Vha44-expressing tissue and that Wg signaling is moderately upregulated upon Vha44 overexpression (supplementary material Fig. S7F,K). Increased proliferation at tissue boundaries is particularly interesting because mechanical strains at the boundary can lead to overcrowding, which has recently been shown to cause delamination and apoptosis (Marinari et al., 2012). These effects possibly play a role when Vha44 is expressed in the *ptc* domain. Here, cells become strongly apoptotic and are basally excluded close to the boundary. Upon inhibition of apoptosis, the proliferation effect induced by Vha44 becomes visible and might be further supported by the release of growth factors from the transformed cells themselves or from the tissue environment. Beyond developmental boundaries, such as the AP boundary, it is conceivable that *in situ* carcinomas can generate similar border effects (Vidal et al., 2006; Vidal et al., 2010).

Vha44-induced tumorigenesis depends on Ras and JNK signaling

A major advantage of *Drosophila* for studying cancer-related processes is the introduction of multiple genetic alterations. Genetic interaction experiments are very useful for assessing the cooperativity of oncogenic pathways. Such studies have highlighted the importance of Ras signaling in eliciting cancerous transformation upon defects in epithelial polarity and membrane trafficking (Pagliarini and Xu, 2003; Chi et al., 2010). Although poorly understood, the JNK signaling pathway seems to play a central role in this process (Igaki et al., 2006; Uhlirova and Bohmann, 2006; Leong et al., 2009; Wu et al., 2010). One example is the RasV12-induced shift of the JNK activating ligand, Eiger/TNF-alpha, from a tumor suppressor into a tumor promoter (Cordero et al., 2010). Whether the increase of invasion and overgrowth by RasV12 in our tumor model involves JNK signaling and whether the activation of JNK by Vha44 requires Ras remains to be further explored. It also needs to be determined how Eiger/JNK inhibition rescues the pathological aspects of our model. The inhibition of apoptosis might be the prime reason for the rescue, but more direct influences on the endolysosomal or associated pathways, such as autophagy, cannot be excluded at this stage (Wu et al., 2009).

Conclusions

Here, we introduce a novel tumor model in *Drosophila* based on V-ATPase subunit C overexpression. We describe the induction of cellular transformation in the native epithelium, with high similarity to human cancers. Genetic dissection of our model revealed increased endosomal acidification, disrupted endolysosomal trafficking and degradation as well as a requirement for JNK signaling. All these effects have previously not been associated with V-ATPase overexpression in tumors. A recent study by Vidal and colleagues showed that sections of human squamous cell carcinoma boundaries exhibited similarities with the wing disc invasion model, including the upregulation of MMPs (Vidal et al., 2010). Due to the elevated levels of ATP6V1C1 in oral squamous cell carcinomas (Otero-Rey et al., 2008), our study suggests that clinical cancer trials involving V-ATPase inhibitors could be expanded to include this type of tumor (Fais, 2010). As demonstrated by the genetic interaction with Ras signaling, our model could also be used for studying the cooperativity of oncogenic pathways and for the evaluation of combinatorial therapies.

MATERIALS AND METHODS

Fly stocks

For Vha44 expression in the wing disc, we used *ptc*-Gal4, *dpp*-Gal4, *nub*-GAL4 (all Bloomington) or *ap*-Gal4 (a gift of Marek Mlodzik) drivers. Controls for UAS-Vha44-HA or UAS-Vha44 were UAS-myr-mRFP or UAS-GFP (both Bloomington). Apoptosis inhibition was performed by coexpression of UAS-p35 (Bloomington). As JNK reporter we used *puc-lacZ (E69)*, which also acts as a mild JNK activator. The basal membrane was visualized with viking-GFP (Flytrap). Other flystocks were: *egr*^{3} (a gift of Marcos Vidal), UAS-Nhe2-YFP (Simons et al., 2009), UAS-puc2A, UAS-Bsk-DN (both a gift of Stephane Noselli), *E(Spl)β -lacZ* (a gift of Eric Lai) and UAS-Vha100-1 (a gift of Robin Hiesinger). Flies were raised and crossed at 25°C, except for p35 or *ap*-GAL4 crosses at 29°C. For the generation of the UAS-Vha44 and the UAS-Vha44-HA fly strains we cloned Vha44 with the following primers: forward, 5′-CACCATGATGTCGGAATACT-3′ and reverse, 5′-TTAGAC-CTTGGCCTGCTCCA-3′ (with STOP codon for Vha44) or reverse, 5′-GACCTTGGCCTGCTCCACCA-3′ (without STOP codon for Vha44-HA). The amplicon was first inserted into the pENTR^{TM}/SD/D-TOPO$^{®}$ Gateway vector (Invitrogen) and then cloned into the pUASg-attB or pUASg-HA-attB destination vectors (kindly provided by Konrad Basler). Transgenesis was performed by Bestgene, Inc.

Antibody and dye stainings

Wing discs were dissected from L3 larvae in PBS and immunostained according to standard procedures (Hermle et al., 2010). Antibodies and dyes used in this study were: mouse anti-Dlg (1:25), rat anti-DE-cadherin (1:25), mouse anti-Notch (NICD) (1:50), mouse anti-Notch (NECD) (1:50), mouse anti-Wg (1:50), mouse anti-MMP1 (1:25), mouse anti-b-gal (1:25; all from DSHB), rat anti-HA (1:200; from Roche), rabbit anti-cleaved Caspase 3 (1:200; from Cell Signaling), rabbit anti-Laminin (1:25; from Abcam), rabbit anti-Rab7 (1:1000; kindly provided by Akira Nakamura), rabbit anti-Avl (1:250; kindly provided by David Bilder), guinea pig anti-v100 (1:2000; kindly provided by Robin Hiesinger), mouse anti-pJNK (G7) (1:50; from Santa Cruz Biotechnology); rabbit anti-pAbl[pY412] (1:100; from Invitrogen). A polyclonal antibody against Vha44 was raised in guinea pig against the following peptide: QIGQIDGDLKTKSQA (Eurogentec). For F-actin and nuclei visualization, AlexaFluor 488- and 555-Phalloidin (1:1000; from Invitrogen) and HOE33342 (1:1000; from Invitrogen) were used, respectively. For TUNEL staining, wing discs were dissected in PBS, fixed in 4% paraformaldehyde and permeabilized. The Fluorescein *In Situ* Cell Death Detection Kit (Roche) was used according to the instruction manual. To assess intravesicular acidification, dissected L3 larval discs were incubated for 2 minutes at room temperature with LysoTracker green DND26 or red DND99 (1 μM; Invitrogen) in PBS, then mounted and immediately analyzed. V-ATPase activity was blocked with Concanamycin A (1 μM; Sigma) treatment for 3 hours at room temperature in PBS. Notch internalization assays were performed as described (Vaccari and Bilder, 2005). Discs were analyzed by Zeiss LSM 510 laser confocal microscopy. Images were processed with Adobe Photoshop and ImageJ software. For quantification, the area of the Cas3- or mRFP-positive cells was determined and normalized to the area of the *ptc* stripe. The mean pixel intensities of the

immunoreactive Rab7 signal were measured in square areas of equal size in Vha44-expressing and neighboring wild-type tissue.

Western blotting

A total of 15 wing discs for each genotype were dissected and immediately lysed in cold RIPA buffer. The whole disc extract was loaded on 12% SDS-PAGE gel and western blot was performed following standard procedures. The Vha44 antibody was used at 1:500. Other antibodies were anti-β-tubulin (1:1000; from DSHB) and horseradish peroxidase (HRP)-conjugated anti-guinea pig and anti-mouse (1:5000; from Santa Cruz Biotechnology and DAKO, respectively).

Quantitative RT-PCR

Total RNA from wing imaginal discs expressing (40 discs per sample) was extracted using TRIZOL Reagent (Invitrogen) and RNeasy Mini Kit (Qiagen) according to the manufacturer's protocol. Concentration and purity was determined by measuring optical density at 260 and 280 nm using a Nanodrop spectrophotometer. 500 µg of total RNA was reverse transcribed using a SuperScript VILO cDNA Synthesis kit (Invitrogen) according to the manufacturer's protocol. 5 ng of cDNA was amplified (in triplicate) in a reaction volume of 15 µl containing the following reagents: 7.5 µl of TaqMan PCR Mastermix 2× No UNG (Applied Biosystems, Foster City, CA), 0.75 µl of TaqMan Gene expression assay 20× (Applied Biosystems, Foster City, CA). 300 nM of primers and 100 nM of Roche probes were used for each sample. RT-PCR was carried out on the ABI/Prism 7900 HT Sequence Detector System (Applied Biosystems), using a pre-PCR step of 10 minutes at 95°C, followed by 40 cycles of 15 seconds at 95°C and 60 seconds at 60°C.

The following primers were used: forward, 5′-GAGTGCCTGACCCAGGAG-3′ and reverse, 5′-CGGTCAGCTCCAGGATGT-3′ [for *E(spl)mβ*]; forward, 5′-GTCACACCAATCAGTGGAG-3′ and reverse, 5′-CGAGCAGCCGGATTCTATTA-3′ (for fz3); forward, 5′-GCCACATCAGAACATCAAGC-3′ and reverse, 5′-CCGTTTTCCGTGCATCTT-3′ (for *puc*); forward, 5′-CGGATCGATATGCTAAGCTGT-3′ and reverse, 5′-CGACGCACTCTGTTGTCG-3′ (for rpL32-RA).

Data were analyzed using GraphPad Prism 5.0d (GraphPad Software). Values were normalized by the amount of *rpl32* in each sample. Statistical analysis was performed using the Student's *t*-test.

ACKNOWLEDGEMENTS

We thank Susanne Helmstädter for excellent technical support. We thank G. Pyrowolakis, M. Mlodzik, M. Vidal, T. Xu, S. Noselli, R. Rousset, Flytrap, the Bloomington Stock Center and the VDRC for fly strains. We thank the DHSB for antibodies, as well as A. Nakamura and D. Bilder for antibodies. We acknowledge Roland Nitschke from the Life Imaging Center Freiburg for help with confocal microscopy. We thank M. Vidal and M. Norman for helpful suggestions and the critical reading of the manuscript.

COMPETING INTERESTS

The authors declare that they do not have any competing or financial interests.

AUTHOR CONTRIBUTIONS

A.G.P. and M.S. conceived the project based on the initial observation of the Vha44 phenotype. A.G.P., E.M.G. and A.F. designed and performed the experiments and analyzed the data. T.V. and M.S. designed the experiments and analyzed the data. T.V. and M.S. wrote the manuscript. All authors read, discussed and edited the manuscript.

FUNDING

A.G.P., E.M.G. and M.S. are supported by an Emmy-Noether grant [grant number SI1303/2-1] by the Deutsche Forschungsgemeinschaft and by the Bundesministerium für Bildung und Forschung (Gerontosys-NephAge). A.F. and T.V. are supported by a new unit start-up grant from Associazione Italiana Ricerca contro il Cancro.

SUPPLEMENTARY MATERIAL

Supplementary material for this article is available at http://dmm.biologists.org/lookup/suppl/doi:10.1242/dmm.010660/-/DC1

REFERENCES

Buechling, T., Bartscherer, K., Ohkawara, B., Chaudhary, V., Spirohn, K., Niehrs, C. and Boutros, M. (2010). Wnt/Frizzled signaling requires dPRR, the Drosophila homolog of the prorenin receptor. *Curr. Biol.* **20**, 1263-1268.

Chi, C., Zhu, H., Han, M., Zhuang, Y., Wu, X. and Xu, T. (2010). Disruption of lysosome function promotes tumor growth and metastasis in Drosophila. *J. Biol. Chem.* **285**, 21817-21823.

Cordero, J. B., Macagno, J. P., Stefanatos, R. K., Strathdee, K. E., Cagan, R. L. and Vidal, M. (2010). Oncogenic Ras diverts a host TNF tumor suppressor activity into tumor promoter. *Dev. Cell* **18**, 999-1011.

Cruciat, C. M., Ohkawara, B., Acebron, S. P., Karaulanov, E., Reinhard, C., Ingelfinger, D., Boutros, M. and Niehrs, C. (2010). Requirement of prorenin receptor and vacuolar H+-ATPase-mediated acidification for Wnt signaling. *Science* **327**, 459-463.

D'Souza, S., Garcia-Cabado, A., Yu, F., Teter, K., Lukacs, G., Skorecki, K., Moore, H. P., Orlowski, J. and Grinstein, S. (1998). The epithelial sodium-hydrogen antiporter Na+/H+ exchanger 3 accumulates and is functional in recycling endosomes. *J. Biol. Chem.* **273**, 2035-2043.

Diab, H., Ohira, M., Liu, M., Cobb, E. and Kane, P. M. (2009). Subunit interactions and requirements for inhibition of the yeast V1-ATPase. *J. Biol. Chem.* **284**, 13316-13325.

Fais, S. (2010). Proton pump inhibitor-induced tumour cell death by inhibition of a detoxification mechanism. *J. Intern. Med.* **267**, 515-525.

Feng, S., Deng, L., Chen, W., Shao, J., Xu, G. and Li, Y. P. (2009). Atp6v1c1 is an essential component of the osteoclast proton pump and in F-actin ring formation in osteoclasts. *Biochem. J.* **417**, 195-203.

Forgac, M. (2007). Vacuolar ATPases: rotary proton pumps in physiology and pathophysiology. *Nat. Rev. Mol. Cell Biol.* **8**, 917-929.

García-García, A., Pérez-Sayáns García, M., Rodríguez, M. J., Antúnez-López, J., Barros-Angueira, F., Somoza-Martín, M., Gándara-Rey, J. M. and Aguirre-Urízar, J. M. (2012). Immunohistochemical localization of C1 subunit of V-ATPase (ATPase C1) in oral squamous cell cancer and normal oral mucosa. *Biotech. Histochem.* **87**, 133-139.

Halder, G. and Mills, G. B. (2011). Drosophila in cancer research: to boldly go where no one has gone before. *Oncogene* **30**, 4063-4066.

Hay, B. A., Wolff, T. and Rubin, G. M. (1994). Expression of baculovirus P35 prevents cell death in Drosophila. *Development* **120**, 2121-2129.

Hermle, T., Saltukoglu, D., Grünewald, J., Walz, G. and Simons, M. (2010). Regulation of Frizzled-dependent planar polarity signaling by a V-ATPase subunit. *Curr. Biol.* **20**, 1269-1276.

Hermle, T., Guida, M. C., Beck, S., Helmstadter, S. and Simons, M. (2013). Drosophila ATP6AP2/VhaPRR functions both as a novel planar cell polarity core protein and a regulator of endosomal trafficking. *EMBO J.* **32**, 245-259.

Hinton, A., Bond, S. and Forgac, M. (2009). V-ATPase functions in normal and disease processes. *Pflugers Arch.* **457**, 589-598.

Hori, K., Sen, A., Kirchhausen, T. and Artavanis-Tsakonas, S. (2011). Synergy between the ESCRT-III complex and Deltex defines a ligand-independent Notch signal. *J. Cell Biol.* **195**, 1005-1015.

Hughes, A. L. and Gottschling, D. E. (2012). An early age increase in vacuolar pH limits mitochondrial function and lifespan in yeast. *Nature* **492**, 261-265.

Huh, J. R., Guo, M. and Hay, B. A. (2004). Compensatory proliferation induced by cell death in the Drosophila wing disc requires activity of the apical cell death caspase Dronc in a nonapoptotic role. *Curr. Biol.* **14**, 1262-1266.

Hurtado-Lorenzo, A., Skinner, M., El Annan, J., Futai, M., Sun-Wada, G. H., Bourgoin, S., Casanova, J., Wildeman, A., Bechoua, S., Ausiello, D. A. et al. (2006). V-ATPase interacts with ARNO and Arf6 in early endosomes and regulates the protein degradative pathway. *Nat. Cell Biol.* **8**, 124-136.

Huss, M., Vitavska, O., Albertmelcher, A., Bockelmann, S., Nardmann, C., Tabke, K., Tiburcy, F. and Wieczorek, H. (2011). Vacuolar H(+)-ATPases: intra- and intermolecular interactions. *Eur. J. Cell Biol.* **90**, 688-695.

Igaki, T., Kanda, H., Yamamoto-Goto, Y., Kanuka, H., Kuranaga, E., Aigaki, T. and Miura, M. (2002). Eiger, a TNF superfamily ligand that triggers the Drosophila JNK pathway. *EMBO J.* **21**, 3009-3018.

Igaki, T., Pagliarini, R. A. and Xu, T. (2006). Loss of cell polarity drives tumor growth and invasion through JNK activation in Drosophila. *Curr. Biol.* **16**, 1139-1146.

Igaki, T., Pastor-Pareja, J. C., Aonuma, H., Miura, M. and Xu, T. (2009). Intrinsic tumor suppression and epithelial maintenance by endocytic activation of Eiger/TNF signaling in Drosophila. *Dev. Cell* **16**, 458-465.

Igaki, T., Kanda, H., Okano, H., Xu, T. and Miura, M. (2011). Eiger and wengen: the Drosophila orthologs of TNF/TNFR. *Adv. Exp. Med. Biol.* **691**, 45-50.

Jefferies, K. C. and Forgac, M. (2008). Subunit H of the vacuolar (H+) ATPase inhibits ATP hydrolysis by the free V1 domain by interaction with the rotary subunit F. *J. Biol. Chem.* **283**, 4512-4519.

Kane, P. M. (2000). Regulation of V-ATPases by reversible disassembly. *FEBS Lett.* **469**, 137-141.

Landsberg, K. P., Farhadifar, R., Ranft, J., Umetsu, D., Widmann, T. J., Bittig, T., Said, A., Jülicher, F. and Dahmann, C. (2009). Increased cell bond tension governs cell sorting at the Drosophila anteroposterior compartment boundary. *Curr. Biol.* **19**, 1950-1955.

Leong, G. R., Goulding, K. R., Amin, N., Richardson, H. E. and Brumby, A. M. (2009). Scribble mutants promote aPKC and JNK-dependent epithelial neoplasia independently of Crumbs. *BMC Biol.* **7**, 62.

Lu, X., Qin, W., Li, J., Tan, N., Pan, D., Zhang, H., Xie, L., Yao, G., Shu, H., Yao, M. et al. (2005). The growth and metastasis of human hepatocellular carcinoma xenografts are inhibited by small interfering RNA targeting to the subunit ATP6L of proton pump. *Cancer Res.* **65**, 6843-6849.

Marinari, E., Mehonic, A., Curran, S., Gale, J., Duke, T. and Baum, B. (2012). Live-cell delamination counterbalances epithelial growth to limit tissue overcrowding. *Nature* **484**, 542-545.

Merzendorfer, H., Reineke, S., Zhao, X. F., Jacobmeier, B., Harvey, W. R. and Wieczorek, H. (2000). The multigene family of the tobacco hornworm V-ATPase: novel subunits a, C, D, H, and putative isoforms. *Biochim. Biophys. Acta* **1467**, 369-379.

Moberg, K. H., Schelble, S., Burdick, S. K. and Hariharan, I. K. (2005). Mutations in erupted, the Drosophila ortholog of mammalian tumor susceptibility gene 101, elicit non-cell-autonomous overgrowth. *Dev. Cell* **9**, 699-710.

Morata, G., Shlevkov, E. and Pérez-Garijo, A. (2011). Mitogenic signaling from apoptotic cells in Drosophila. *Dev. Growth Differ.* **53**, 168-176.

Moreno, E., Yan, M. and Basler, K. (2002). Evolution of TNF signaling mechanisms: JNK-dependent apoptosis triggered by Eiger, the Drosophila homolog of the TNF superfamily. *Curr. Biol.* **12**, 1263-1268.

Niehrs, C. and Boutros, M. (2010). Trafficking, acidification, and growth factor signaling. *Sci. Signal.* **3**, pe26.

Nishisho, T., Hata, K., Nakanishi, M., Morita, Y., Sun-Wada, G. H., Wada, Y., Yasui, N. and Yoneda, T. (2011). The a3 isoform vacuolar type H^+-ATPase promotes distant metastasis in the mouse B16 melanoma cells. *Mol. Cancer Res.* **9**, 845-855.

Otero-Rey, E. M., Somoza-Martín, M., Barros-Angueira, F. and García-García, A. (2008). Intracellular pH regulation in oral squamous cell carcinoma is mediated by increased V-ATPase activity via over-expression of the ATP6V1C1 gene. *Oral Oncol.* **44**, 193-199.

Pagliarini, R. A. and Xu, T. (2003). A genetic screen in Drosophila for metastatic behavior. *Science* **302**, 1227-1231.

Pérez-Garijo, A., Martín, F. A. and Morata, G. (2004). Caspase inhibition during apoptosis causes abnormal signalling and developmental aberrations in Drosophila. *Development* **131**, 5591-5598.

Pérez-Sayáns, M., García-García, A., Reboiras-López, M. D. and Gándara-Vila, P. (2009). Role of V-ATPases in solid tumors: importance of the subunit C (Review). *Int. J. Oncol.* **34**, 1513-1520.

Pulipparacharuvil, S., Akbar, M. A., Ray, S., Sevrioukov, E. A., Haberman, A. S., Rohrer, J. and Krämer, H. (2005). Drosophila Vps16A is required for trafficking to lysosomes and biogenesis of pigment granules. *J. Cell Sci.* **118**, 3663-3673.

Puopolo, K., Sczekan, M., Magner, R. and Forgac, M. (1992). The 40-kDa subunit enhances but is not required for activity of the coated vesicle proton pump. *J. Biol. Chem.* **267**, 5171-5176.

Robey, I. F., Baggett, B. K., Kirkpatrick, N. D., Roe, D. J., Dosescu, J., Sloane, B. F., Hashim, A. I., Morse, D. L., Raghunand, N., Gatenby, R. A. et al. (2009). Bicarbonate increases tumor pH and inhibits spontaneous metastases. *Cancer Res.* **69**, 2260-2268.

Rodahl, L. M., Haglund, K., Sem-Jacobsen, C., Wendler, F., Vincent, J. P., Lindmo, K., Rusten, T. E. and Stenmark, H. (2009). Disruption of Vps4 and JNK function in Drosophila causes tumour growth. *PLoS ONE* **4**, e4354.

Rohrer, J., Schweizer, A., Russell, D. and Kornfeld, S. (1996). The targeting of Lamp1 to lysosomes is dependent on the spacing of its cytoplasmic tail tyrosine sorting motif relative to the membrane. *J. Cell Biol.* **132**, 565-576.

Rong, Y., McPhee, C. K., Deng, S., Huang, L., Chen, L., Liu, M., Tracy, K., Baehrecke, E. H., Yu, L. and Lenardo, M. J. (2011). Spinster is required for autophagic lysosome reformation and mTOR reactivation following starvation. *Proc. Natl. Acad. Sci. USA* **108**, 7826-7831.

Ryoo, H. D., Gorenc, T. and Steller, H. (2004). Apoptotic cells can induce compensatory cell proliferation through the JNK and the Wingless signaling pathways. *Dev. Cell* **7**, 491-501.

Sennoune, S. R., Bakunts, K., Martínez, G. M., Chua-Tuan, J. L., Kebir, Y., Attaya, M. N. and Martínez-Zaguilán, R. (2004). Vacuolar H+-ATPase in human breast cancer cells with distinct metastatic potential: distribution and functional activity. *Am. J. Physiol. Cell Physiol.* **286**, C1443-C1452.

Simons, M., Gault, W. J., Gotthardt, D., Rohatgi, R., Klein, T. J., Shao, Y., Lee, H. J., Wu, A. L., Fang, Y., Satlin, L. M. et al. (2009). Electrochemical cues regulate assembly of the Frizzled/Dishevelled complex at the plasma membrane during planar epithelial polarization. *Nat. Cell Biol.* **11**, 286-294.

Singh, J., Aaronson, S. A. and Mlodzik, M. (2010). Drosophila Abelson kinase mediates cell invasion and proliferation through two distinct MAPK pathways. *Oncogene* **29**, 4033-4045.

Stock, C. and Schwab, A. (2009). Protons make tumor cells move like clockwork. *Pflugers Arch.* **458**, 981-992.

Thompson, B. J., Mathieu, J., Sung, H. H., Loeser, E., Rørth, P. and Cohen, S. M. (2005). Tumor suppressor properties of the ESCRT-II complex component Vps25 in Drosophila. *Dev. Cell* **9**, 711-720.

Uhlirova, M. and Bohmann, D. (2006). JNK- and Fos-regulated Mmp1 expression cooperates with Ras to induce invasive tumors in Drosophila. *EMBO J.* **25**, 5294-5304.

Vaccari, T. and Bilder, D. (2005). The Drosophila tumor suppressor vps25 prevents nonautonomous overproliferation by regulating notch trafficking. *Dev. Cell* **9**, 687-698.

Vaccari, T., Lu, H., Kanwar, R., Fortini, M. E. and Bilder, D. (2008). Endosomal entry regulates Notch receptor activation in Drosophila melanogaster. *J. Cell Biol.* **180**, 755-762.

Vaccari, T., Duchi, S., Cortese, K., Tacchetti, C. and Bilder, D. (2010). The vacuolar ATPase is required for physiological as well as pathological activation of the Notch receptor. *Development* **137**, 1825-1832.

Vidal, M., Larson, D. E. and Cagan, R. L. (2006). Csk-deficient boundary cells are eliminated from normal Drosophila epithelia by exclusion, migration, and apoptosis. *Dev. Cell* **10**, 33-44.

Vidal, M., Salavaggione, L., Ylagan, L., Wilkins, M., Watson, M., Weilbaecher, K. and Cagan, R. (2010). A role for the epithelial microenvironment at tumor boundaries: evidence from Drosophila and human squamous cell carcinomas. *Am. J. Pathol.* **176**, 3007-3014.

Voss, M., Vitavska, O., Walz, B., Wieczorek, H. and Baumann, O. (2007). Stimulus-induced phosphorylation of vacuolar H(+)-ATPase by protein kinase A. *J. Biol. Chem.* **282**, 33735-33742.

Webb, B. A., Chimenti, M., Jacobson, M. P. and Barber, D. L. (2011). Dysregulated pH: a perfect storm for cancer progression. *Nat. Rev. Cancer* **11**, 671-677.

Wilkin, M., Tongngok, P., Gensch, N., Clemence, S., Motoki, M., Yamada, K., Hori, K., Taniguchi-Kanai, M., Franklin, E., Matsuno, K. et al. (2008). Drosophila HOPS and AP-3 complex genes are required for a Deltex-regulated activation of notch in the endosomal trafficking pathway. *Dev. Cell* **15**, 762-772.

Wu, H., Wang, M. C. and Bohmann, D. (2009). JNK protects Drosophila from oxidative stress by trancriptionally activating autophagy. *Mech. Dev.* **126**, 624-637.

Wu, M., Pastor-Pareja, J. C. and Xu, T. (2010). Interaction between Ras(V12) and scribbled clones induces tumour growth and invasion. *Nature* **463**, 545-548.

Yan, Y., Denef, N. and Schüpbach, T. (2009). The vacuolar proton pump, V-ATPase, is required for notch signaling and endosomal trafficking in Drosophila. *Dev. Cell* **17**, 387-402.

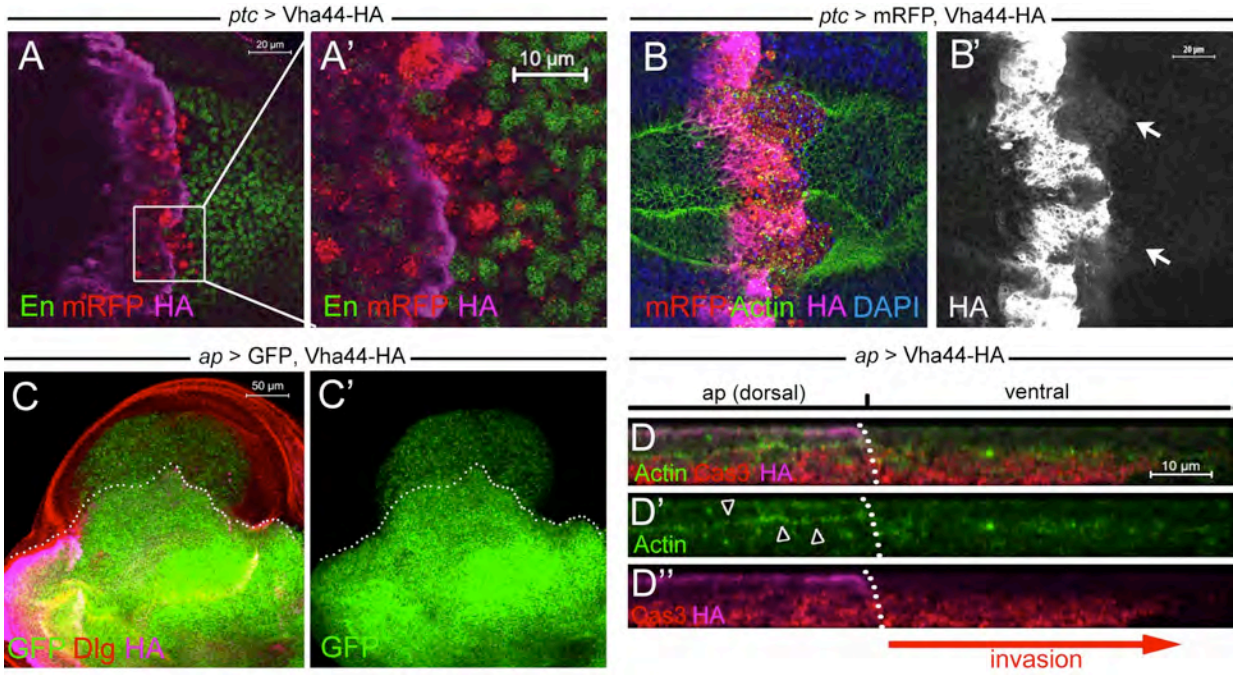

Fig. S1: Invasive behavior upon Vha44 overexpression. (A) Cells overexpressing Vha44-HA and mRFP are not positive for the posterior marker Engrailed (En), suggesting that invasive cells are derived from the *ptc* domain and belong to the anterior compartment. (B) Cells overexpressing Vha44-HA and mRFP lose their HA tag upon invasion into the posterior compartment. Overexposure shows that the HA tag is visible in the invasive front (arrows in A'), albeit to a much lower extent than in the *ptc* stripe. (C) Overexpression of Vha44-HA and GFP in the dorsal part of the wing disc with *ap*-Gal4 causes tissue overgrowth and invasion of GFP-positive cells into the ventral part (D/V boundary is marked with dotted line). (D) X-z-projection of dorsal cells invading across the D/V-boundary (marked with dotted line). Invasive cells display Cas3 reactivity. Arrowheads mark an actin cable that surround the basally extruded and invasive cells.

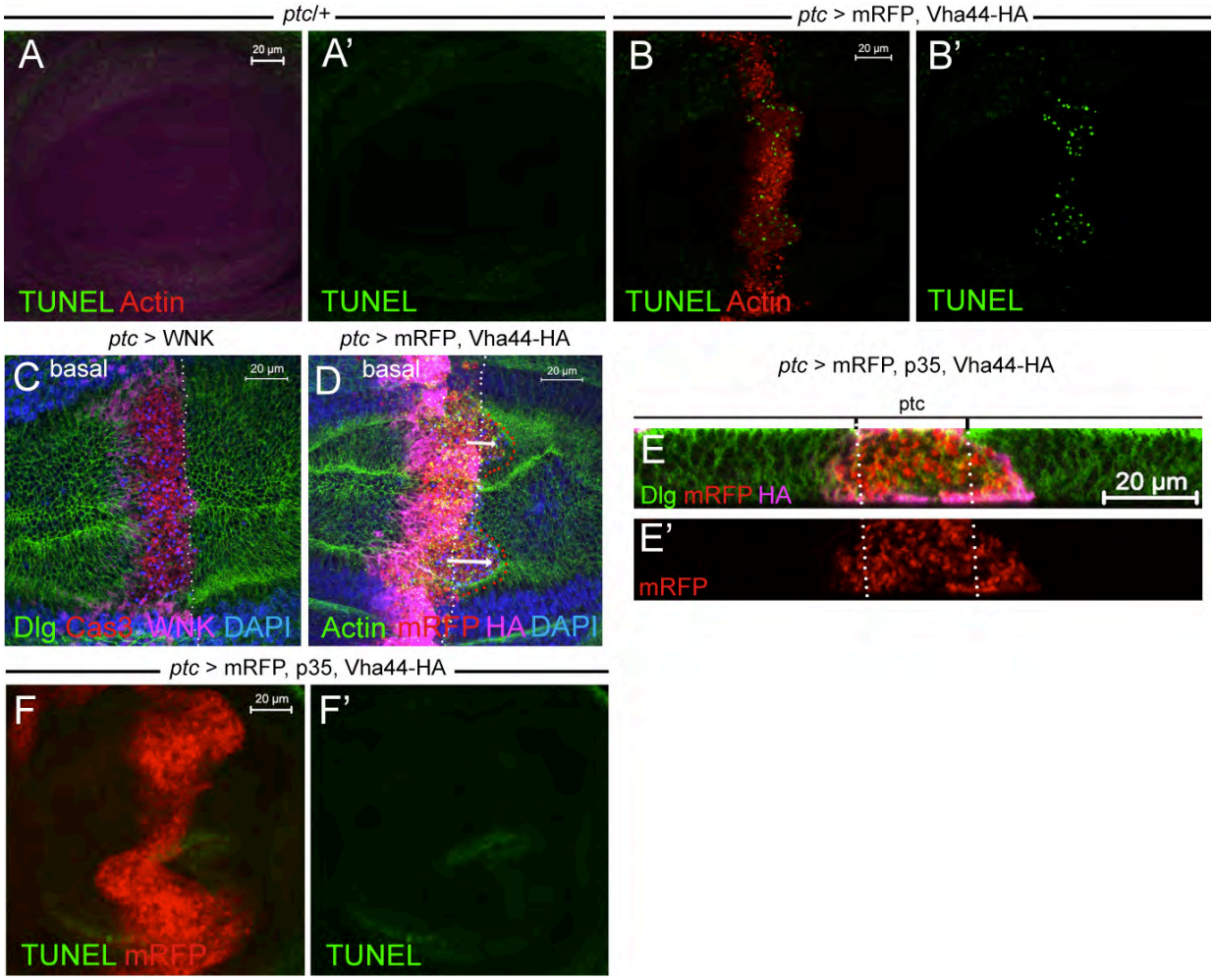

Fig. S2: Vha44 causes cell death in the wing disc. (A) Control discs do not show apoptosis in the *ptc* stripe as assayed with TUNEL staining. (B) Excess Vha44 leads to TUNEL-positive cells in the *ptc* domain. Cas3 staining is shown in Fig. 1. (C,D) Consistent with previous findings (Vidal et al, 2005), triggering apoptosis does not necessarily result in invasive migration. Apoptosis was induced by the *ptc*-GAL4-mediated overexpression of dWNK (CG7177), a kinase that regulates the activity of ion channels (Hoorn et al, 2011). Overexpression of dWNK leads to an increased cell death, as visualized by cleaved Caspase 3. However, no protruding cell masses at the basal AP boundary can be observed (C), as in the case of Vha44-HA (D). (E) X-z-projection of a disc co-expressing p35 and Vha44-HA in the *ptc* stripe (marked with mRFP). p35 co-expression leads to an enlarged and broadened *ptc* stripe. Note that with p35 co-expression the HA tag is now readily visible in all Vha44-HA expressing cells, suggesting that without p35 the HA tag may be cleaved in a caspase-dependent manner (see also Figure 1G'' and G'''). (F,F') Co-expression of p35 abolishes TUNEL staining, confirming the efficiency of p35 as an inhibitor of cell death. The *ptc* stripe appears enlarged and irregular.

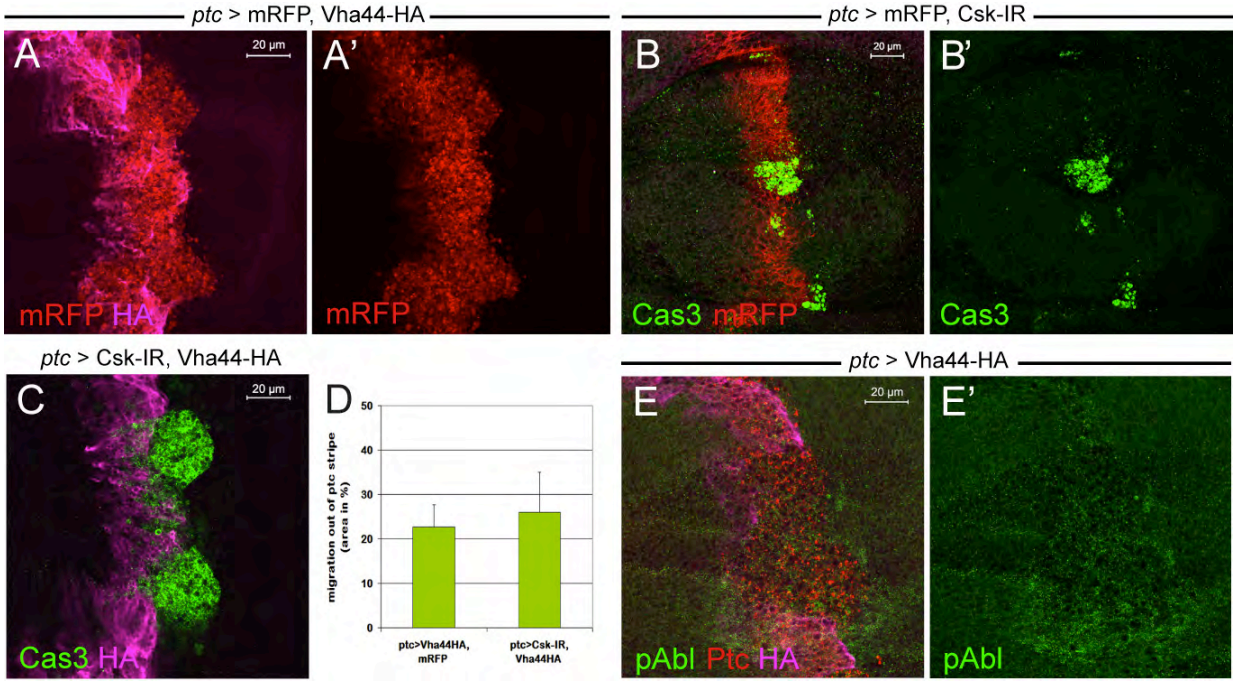

Fig. S3: Vha44-induced invasion does not cooperate with Csk and Abl signaling. (A) The knockdown of the Src inhibitor Csk with *ptc*-GAL4 causes cells to migrate into the posterior compartment. Cells are also Cas3-positive. (B-D) The co-expression of RNAi against Csk and Vha44-HA does not increase the extent of Vha44-induced invasion. UAS-mRFP was used as a control for UAS-Csk-IR. For quantification, the area of the Cas3- or mRFP-positive cells was determined and normalized to the area of the *ptc* stripe. (E) Phospho-Abl is only weakly increased in Vha44 overexpressing cells.

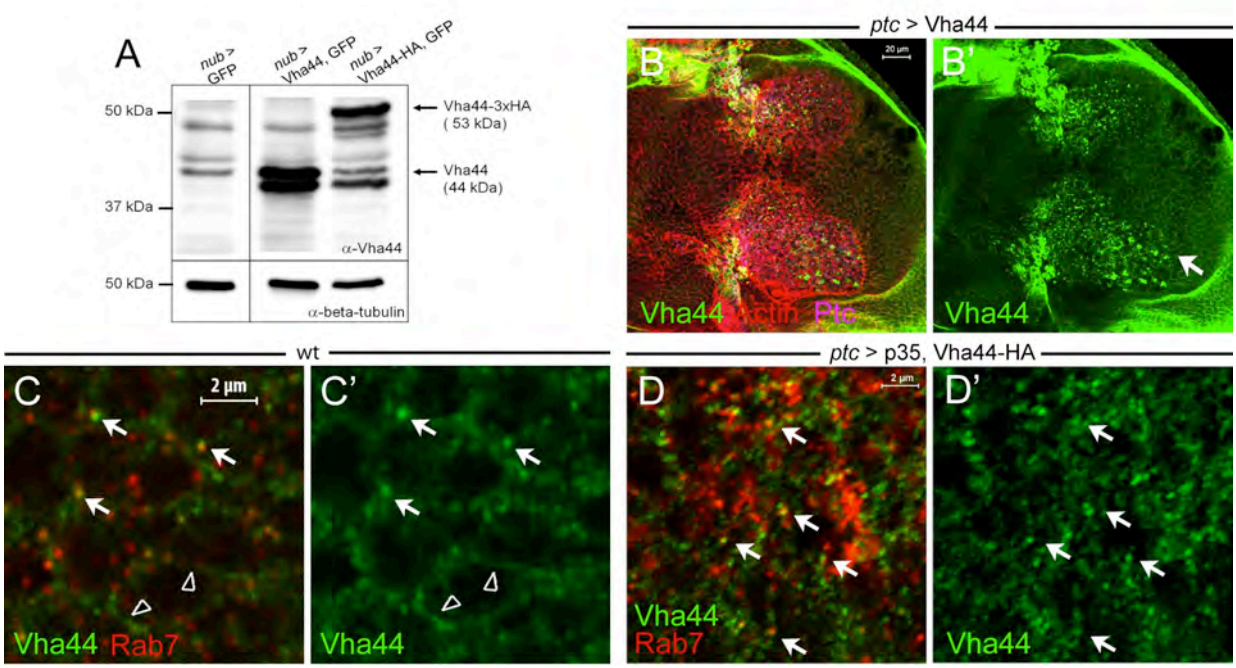

Fig. S4: Subcellular localization of Vha44. (A) Untagged and 3xHA-tagged Vha44 was expressed with *nub*>GAL4. Wing discs were dissected and processed for Western Blot analysis. The Vha44 antibody recognizes a 44 kDa band among other unspecific bands. The 44kDa band is strongly enhanced in the case of Vha44 overexpression. Vha44-3xHA produces a 53 kDa-band, corresponding to the tagged form. In both overexpression lanes, an unidentified additional protein band, just below the 44-kDa band can be seen. (B-D) The Vha44 antibody was also used for visualizing the localization of overexpressed (B,D) and endogenous (C) Vha44 in the wing disc. Unlike the HA antibody (see Figure 1), anti-Vha44 also stains the invasive front (arrow in B'). Endogenous (C) and overexpressed (D) Vha44 show a partial overlap with Rab7-positive compartments (arrows) as well as some plasma membrane localization (arrowheads).

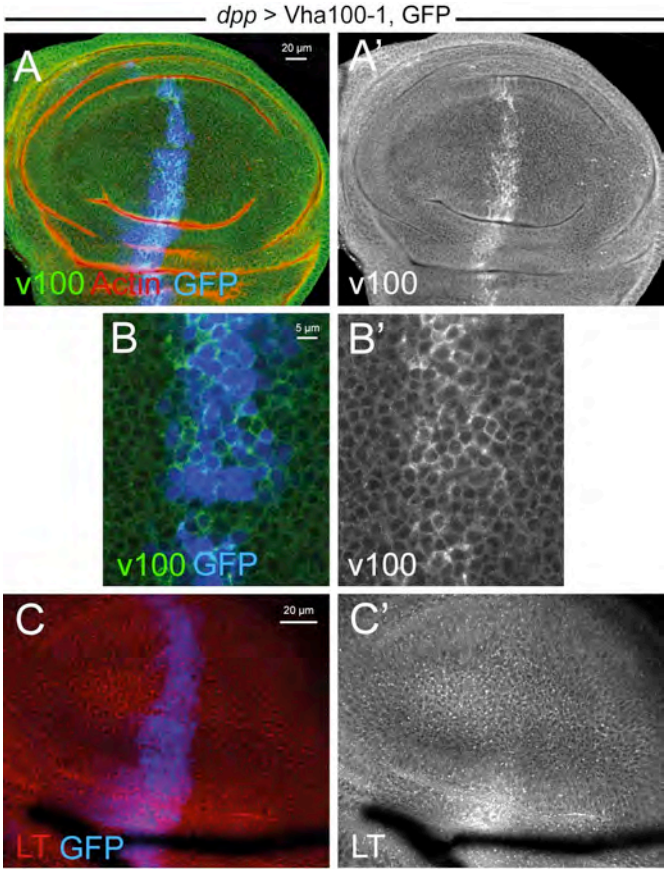

Fig. S5: Vha100-1 overexpression does not cause invasive phenotypes or alter endolysosomal acidification. (A) Overexpression of GFP-tagged V-ATPase subunit Vha100-1 in the *dpp* expression domain can be visualized with anti-v100 antibody and (B) leads to accumulation of v100 at the plasma membrane. In contrast to Vha44 overexpression, Vha100-1 upregulation does not cause invasive phenotypes (A,A,B,B') or an increase in Lysotracker uptake (C,C').

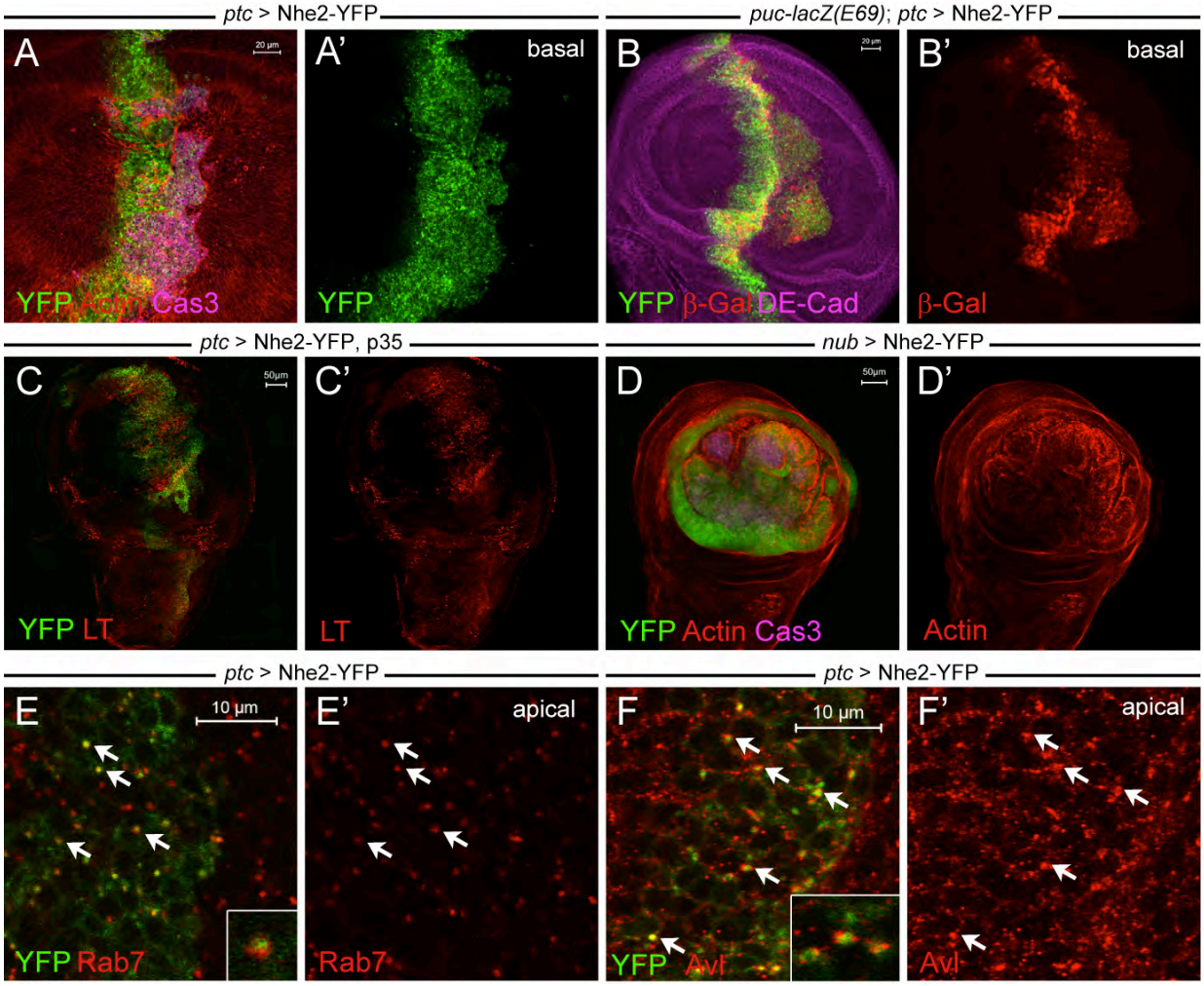

Fig. S6: Nhe2 overexpression phenocopies Vha44 overexpression. *Drosophila* Nhe2 is a sodium-proton exchanger. It has the closest sequence homology to mammalian Nhe3, which that can shuttle between the plasma membrane and endosomal compartments. (A) The overexpression of Nhe2-YFP with *ptc*-GAL4 also causes apoptosis (Cas3 in magenta in A) and invasive migration into the posterior compartment. (B) *Puc-lacZ* expression is activated in Nhe2-expressing cells. (C) Nhe2-YFP overexpression causes increased organellar LysoTracker accumulation both in absence (not shown) and the presence (D) of p35. (D) *nub*-GAL4-mediated Nhe2 expression shows mild overgrowth, recognizable by the bulges in the wing pouch. (E,E',F,F') Upon overexpression with *ptc*-Gal4, Nhe-2 shows partial overlap with Rab7- and Avalanche (Avl)-positive compartments (arrows).

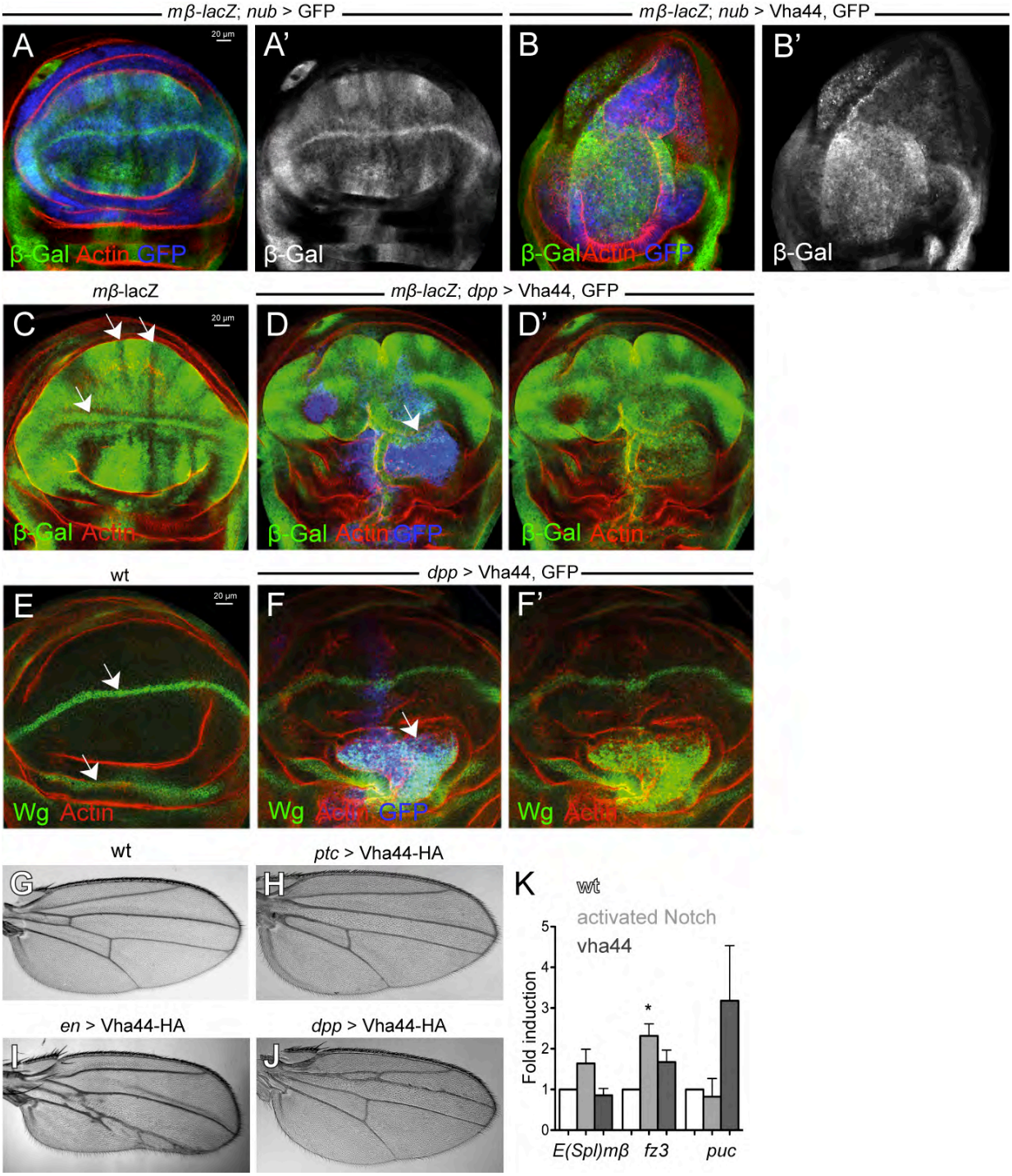

Fig. S7: Vha44 modulates Notch, Wg and JNK signaling. (A) Pattern of expression of the Notch reporter *E(Spl)mβ-lacZ* in the wing pouch. (B) In Vha44 overexpressing cells, the reporter is visible in large portions of the expression domain, indicating persistent signaling activity. (C) Wild-type disc stained for *E(Spl)mβ-lacZ*. Prospective wing veins and margins (here in the disc the dorso-ventral (DV) boundary) are highlighted, in which Notch signaling is usually inactive or very active, respectively. (D) Overexpressing Vha44 in the *dpp* domain causes the loss of the Notch-inactive regions, but the signal increase does not reach the level of peak-signaling regions such as the DV boundary. (E) Control disc showing wild-type (wt) Wg expression pattern along the dorsal-ventral boundary and in the hinge primordium. (F) The overexpression of Vha44 in the *dpp* domain ectopically activates wg expression in a large patch of hinge cells. (G) Wt adult wing (anterior to the top, distal to the right, dorsal facing). (H-J)

Adult wings derived from discs overexpressing Vha44 in the *ptc*, *en (*posterior*)* and *dpp* domains. Note the loss and gain of vein material, which represent established Notch gain- and loss-of-function phenotypes, respectively. (K) Quantitative RT-PCR on wt discs and discs expressing constitutively activated Notch and Vha44 under *nub*-GAL4. The level of expression of *E(spl)mβ*, a Notch signaling target does not significantly change upon Vha44 overexpression. In contrast, the level of *fz3,* a Wg signaling target, is moderately increased upon Vha44 overexpression. This effect is comparable to that of activated Notch signaling, which is upstream of Wg signaling in developing wing imaginal discs. Compared to wt or activated Notch, there is an increased trend for Puc expression in Vha44 overexpressing discs. The panel represents three independent experiments in triplicate. Data are graphed as average and standard deviation relative to wt controls. *$p<0.05$ relative to wild-type.

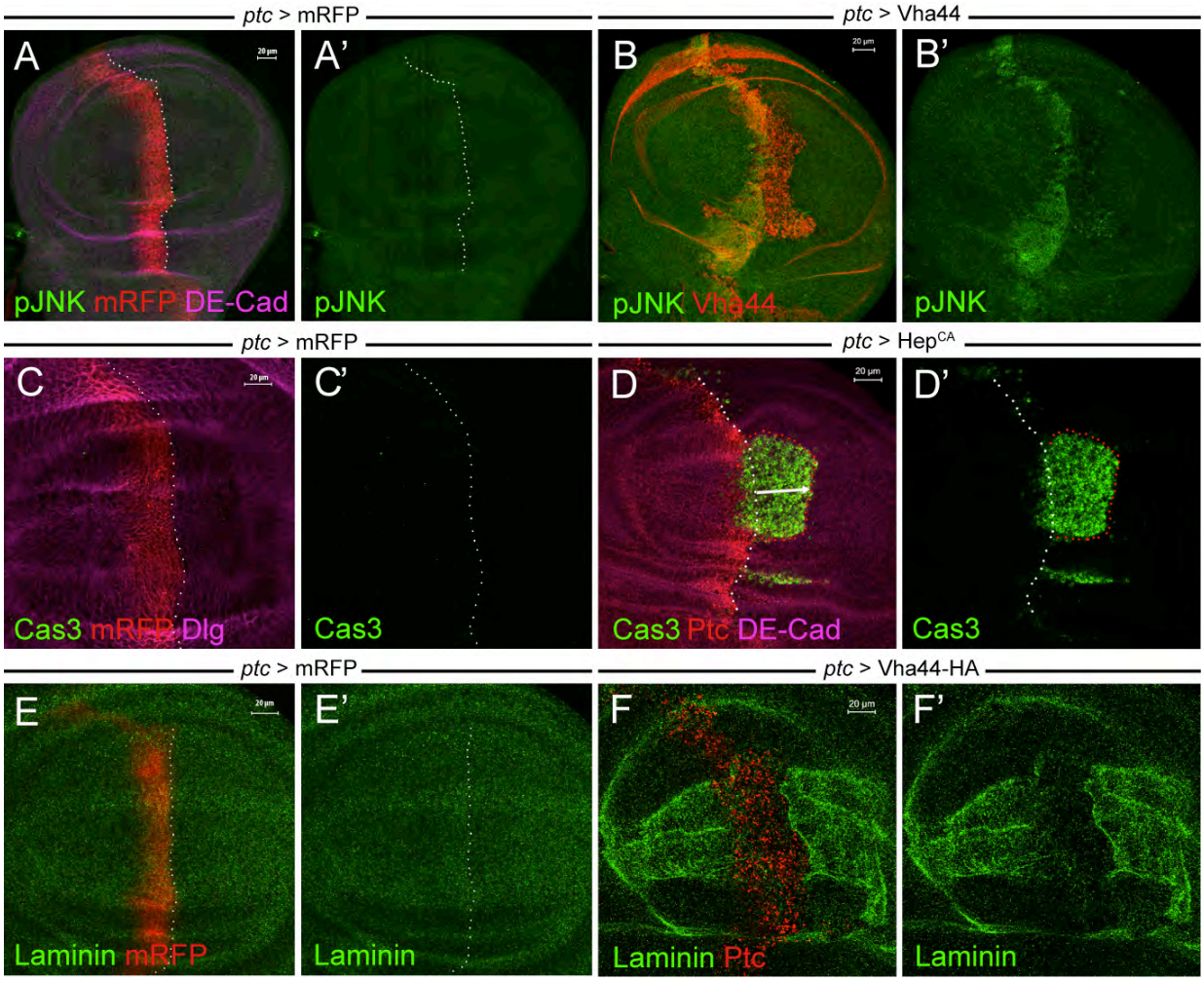

Fig. S8: Vha44 activates JNK signaling and causes ECM degradation. (A) Control discs do not show activation of the JNK pathway in the *ptc* stripe (marked with mRFP) as visualized by Phospho-JNK. (B) Phospho-JNK is visible in the *ptc* expression domain upon Vha44 overexpression. (C) Control discs do not display cleaved Caspase 3-positive cells in the *ptc* stripe (marked with mRFP). (D) Hep^{CA} is the activated form of hemipterous, a JNKK kinase in *Drosophila*. It also leads to invasive cell migration and apoptosis when overexpressed, suggesting that activation of JNK signaling is sufficient to drive invasion. (E) Laminin in control discs is not disturbed in the control *ptc* stripe (marked with mRFP). (F) In agreement with Viking-GFP loss (as shown in Fig. 4), Laminin is lost in basal sections of the *ptc* stripe, most likely due to upregulated activity of proteases such as MMP1.